Role of β-adrenergic signaling in masseter muscle

Aiko Ito[1,2], Yoshiki Ohnuki[1], Kenji Suita[1], Misao Ishikawa[3], Yasumasa Mototani[1], Kouichi Shiozawa[1], Naoya Kawamura[1,4], Yuka Yagisawa[1,2], Megumi Nariyama[5], Daisuke Umeki[2], Yoshiki Nakamura[2], Satoshi Okumura[1] *

1 Department of Physiology, Tsurumi University School of Dental Medicine, Yokohama, Japan,
2 Department of Orthodontics, Tsurumi University School of Dental Medicine, Yokohama, Japan,
3 Department of Oral Anatomy, Tsurumi University School of Dental Medicine, Yokohama, Japan,
4 Department of Periodontology, Tsurumi University School of Dental Medicine, Yokohama, Japan,
5 Department of Pediatric Dentistry, Tsurumi University School of Dental Medicine, Yokohama, Japan

* okumura-s@tsurumi-u.ac.jp

Abstract

In skeletal muscle, the major isoform of β-adrenergic receptor (β-AR) is β_2-AR and the minor isoform is β_1-AR, which is opposite to the situation in cardiac muscle. Despite extensive studies in cardiac muscle, the physiological roles of the β-AR subtypes in skeletal muscle are not fully understood. Therefore, in this work, we compared the effects of chronic β_1- or β_2-AR activation with a specific β_1-AR agonist, dobutamine (DOB), or a specific β_2-AR agonist, clenbuterol (CB), on masseter and cardiac muscles in mice. In cardiac muscle, chronic β_1-AR stimulation induced cardiac hypertrophy, fibrosis and myocyte apoptosis, whereas chronic β_2-AR stimulation induced cardiac hypertrophy without histological abnormalities. In masseter muscle, however, chronic β_1-AR stimulation did not induce muscle hypertrophy, but did induce fibrosis and apoptosis concomitantly with increased levels of p44/42 MAPK (ERK1/2) (Thr-202/Tyr-204), calmodulin kinase II (Thr-286) and mammalian target of rapamycin (mTOR) (Ser-2481) phosphorylation. On the other hand, chronic β_2-AR stimulation in masseter muscle induced muscle hypertrophy without histological abnormalities, as in the case of cardiac muscle, concomitantly with phosphorylation of Akt (Ser-473) and mTOR (Ser-2448) and increased expression of microtubule-associated protein light chain 3-II, an autophagosome marker. These results suggest that the β_1-AR pathway is deleterious and the β_2-AR is protective in masseter muscle. These data should be helpful in developing pharmacological approaches for the treatment of skeletal muscle wasting and weakness.

Introduction

Adrenergic receptors (ARs) belong to the guanine nucleotide-binding G-protein-coupled receptor (GPCR) family. Among them, β_2-AR is the most abundant form in skeletal muscle, while β_1-AR accounts for less than 10% of ARs, and there are small populations of α_1-AR and β_3-AR [1]. In contrast, the predominant receptor subtype expressed in the heart is β_1-AR, with approximately 20% of β_2-AR [2].

The physiological roles of β_1- and β_2-AR in the heart have been extensively investigated using both pharmacological [3,4] and gene-targeting approaches [5]. β_1-AR-mediated cAMP signaling is involved in catecholamine-induced cardiac myocyte hypertrophy in vitro [4] and in vivo [6]. Furthermore, stimulation of β_1-AR triggers cardiac myocyte apoptosis via a cyclic AMP (cAMP)-dependent mechanism [5,7] and maladaptive cardiac remodeling in vivo [8]. In contrast to the well-established deleterious cardiac effects of β_1-AR, β_2-AR stimulation on the heart delivers cardiac hypertrophy with an antiapoptotic effect through the Giα-G$\beta\gamma$-phosphoinositol 3-kinase (PI3K)-Akt cell survival pathway [9,10].

Previous studies of the physiological significance of β-AR signaling in skeletal muscle have focused on the role of β_2-AR stimulation, using selective β_2-AR agonists. Chronic stimulation of β_2-AR with a selective β_2-AR agonist, clenbuterol (CB), induced skeletal muscle hypertrophy via activation of Akt/mechanistc target of rapamycin (mTOR) signaling [11,12], and while histological analysis revealed no abnormality (such as fibrosis), the contractility might be increased, as in the case of cardiac muscle, even though resistance to fatigue was reported to be decreased [11,13–15]. In contrast, the physiological significance of β_1-AR signaling in skeletal muscle remains less extensively investigated, probably due to the low expression level (less than 10% of ARs). But, the physiological importance of β-AR subtypes may depend upon their downstream signaling rather than their expression levels [12].

mTOR regulates cell growth and metabolism via two structurally and functionally distinct mTOR-containing protein complexes, mTORC1 and mTORC2, in response to environmental cues [16]. It was recently reported that mTOR phosphorylation at serine 2448 (mTORC1) is regulated by phosphoinositide 3-kinase (PI3)-Akt signaling and mTOR phosphorylation at serine 2481 (mTORC2) is regulated through the cAMP-PKA pathway in skeletal muscle [11,17]. However, the effects of β-AR subtype-specific stimulation on mTORC1 and mTORC2 remain largely unknown.

Various pathophysiological factors are involved in the progression of muscle dysfunction, including Ca^{2+} homeostasis in skeletal and cardiac muscles [18,19]. The function of the sarcoendoplasmic reticulum (SR) calcium transport ATPase (SERCA2a), a major player in Ca^{2+} homeostasis, is modulated by phospholamban (PLN) in skeletal and cardiac muscles [20]. PLN is a low-molecular weight phosphoprotein in both cardiac and skeletal SR, and dephosphorylated PLN is an inhibitor of SERCA-mediated transport of Ca^{2+}. Thus, PLN plays an important role for the regulation of Ca^{2+} homeostasis in skeletal and cardiac muscle [20]. Following β-AR activation, and thus production of cAMP by adenylyl cyclase, protein kinase A (PKA) phosphorylates PLN on serine 16 and CaMKII phosphorylates PLN on threonine 17 [21]. Importantly, increased PLN phosphorylation or overexpression of PLN exaggerates cardiac function, leading to increased cardiac fibrosis and apoptosis in mice, as established by us and other groups [22–24]. It was recently reported that progressive fibrosis and muscle weakness are induced in mice overexpressing PLN in skeletal muscle [25], but the role of the overexpressed PLN in skeletal muscle is still not clearly understood.

We hypothesized that β_1-AR-mediated signaling and its downstream molecules might play an important role in the development of skeletal muscle dysfunction, and to test this idea, we examined and compared the effects of selective stimulation of β_1- or β_2-AR in masseter muscle and cardiac muscle by chronic infusion of a selective β_1-AR agonist, dobutamine (DOB), or a selective β_2-AR agonist, CB, for 1 week in mice.

Materials and methods

Mice and experimental protocols

All experiments were performed on male 12-week-old C57BL/6 mice obtained from CLEA Japan (Tokyo, Japan). Mice were group-housed at 23°C in under a 12–12 light/dark cycle with
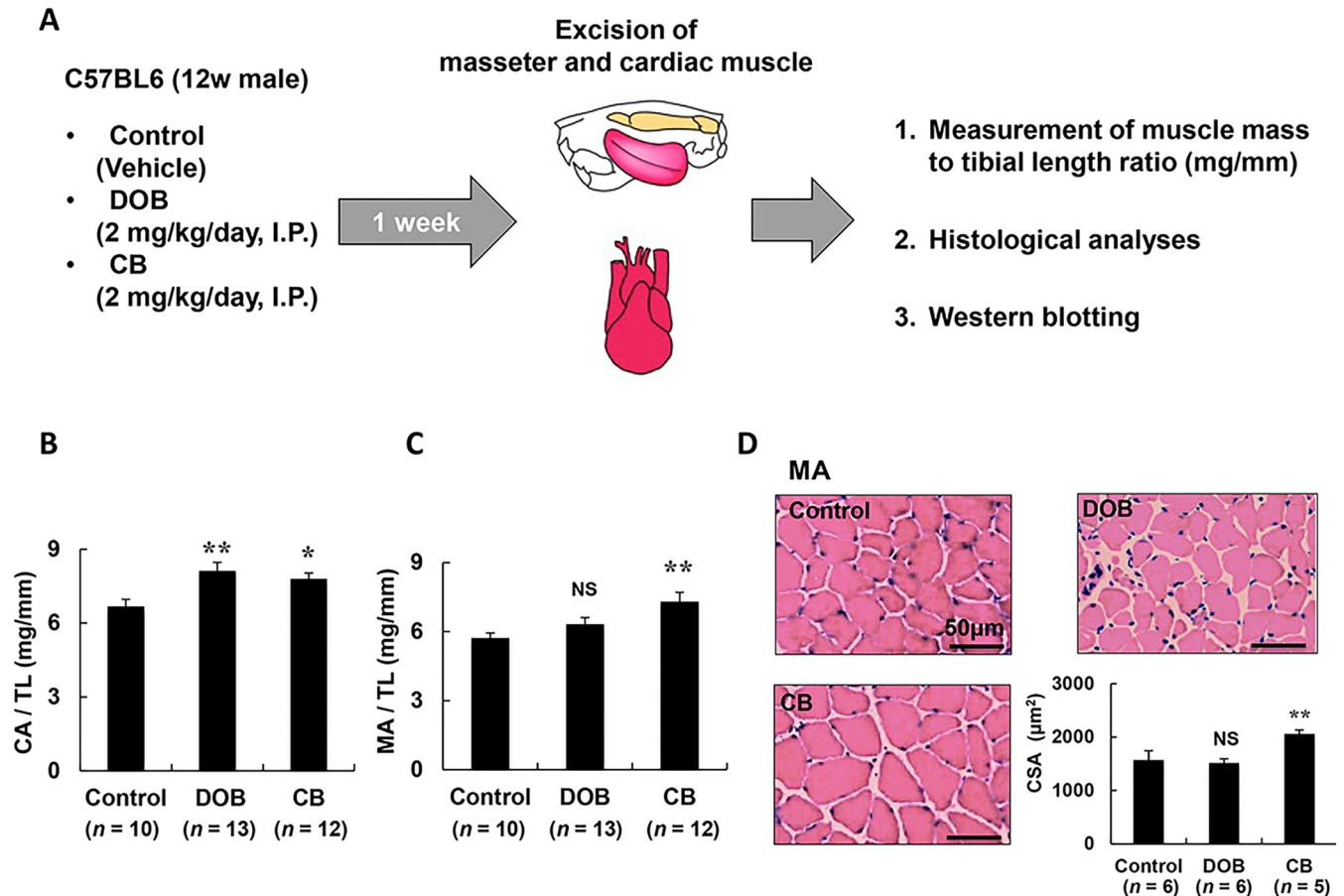
Fig 1. Experimental procedure, daily consumption of food and water, and body weight. (A) Dobutamine (DOB) and clenbuterol (CB) was administered once daily for 1 week via intraperitoneal injection (I.P.) at a dose of 2 mg/kg, dissolved in saline. Age-matched control mice (Control) received an identical volume of saline only. **(B)** In cardiac muscle (CA), the muscle mass per tibial length ratio was significantly increased in the DOB group (**$P < 0.01$ vs. Control), as well as the CB group (*$P < 0.05$ vs. Control). **(C)** In masseter muscle (MA), the muscle mass per tibial length ratio was significantly increased in the CB group (**$P < 0.01$ vs. Control), but not in the DOB group **(D)** Typical cross-sections of HE staining of masseter muscle (MA) in the three groups (Control (*upper left*), DOB (*upper right*) and CB (*lower left*)). CSA was significantly increased in the CB group (**$P < 0.01$ vs. Control), but not in the DOB group (*lower right*). Scale bars: 50 μm.

lights on at 8:00 AM. Food and water were available ad libitum. This study was approved by the Animal Care and Use Committees of Tsurumi University.

DOB (Sigma, St. Louis, MO, USA) and CB (Sigma) were each dissolved in saline to prepare a 0.6 mg/ml stock solution and the appropriate volume of this solution to provide the desired dose (2mg/kg) was added to 0.2 ml of saline to prepare the solution for intraperitoneal (i.p.) injection [11,26]. DOB or CB was administered i.p. once daily for 1 week, while control mice received an identical volume of saline only (**Fig 1A**). β1-AR agonist DOB and β2-AR agonist CB were administered in equal volume doses (2mg/kg) to examine the subtype-specific effects of β-AR in mice, in line with previous studies [11,12,27]. Body weight, food intake, and water intake were monitored for all animals throughout the 1-week experimental period. The dose of CB used in this study has been reported to increase skeletal mass efficiently without affecting body weight [28]. After the completion of each treatment, mice were anesthetized with isoflurane and the heart, left and right masseter muscle were excised, rinsed thoroughly in phosphate-buffered saline (PBS) to eliminate circulating blood in tissue, blotted on filter paper, weighted, frozen, and stored at -80˚C.

The muscle mass (mg) and the ratio of muscle mass to tibial length (mm) were used as indexes of muscle growth. After tissue extraction, the mice were killed by cervical dislocation [29]. The protocol is summarized in **Fig 1A**.

Cross-sectional area of muscle fibers

The left masseter muscle, excised as a whole (**Fig 1A**), was embedded in Tissue-Tek OCT compound (Sakura Finetec, Torrance, CA, USA) in a slightly stretched state so as to maintain a length close to the resting length (L0), and stored at -80˚C until sectioning, as reported [30]. Cross sections (10μm) were cut from the middle portion of the left masseter muscle with a cryostat (CM1900, Leica Microsystems, Nussloch, Germany) at -20˚C. The section were air-dried and fixed with 4% paraformaldehyde in 0.1 M PBS (pH 7.5). The sections were then stained with hematoxylin and eosin (HE) and observed under a light microscope (BX61, Olympus Co., Tokyo, Japan). Micrographs were taken with a digital camera (DP-72, Olympus Co.) connected to a personal computer. The cross-sectional size of muscle fibers was evaluated by measuring the cross-sectional area (CSA) [31,32]. The CSA of 100 muscle fibers in the superficial portion was measured with image analysis software (Image J 1.45) and averaged to obtain the mean values in each mouse.

Evaluation of fibrosis

Among several quantitative methods that are available to determine interstitial fibrotic regions [22,33,34], we employed Masson-trichrome staining using the Accustatin Trichrome Stain Kit (#HT15-1KT; Sigma) in accordance with the manufacturer's protocol, as described previously [22,35]. Interstitial fibrotic regions were quantified using image analysis software (Image J 1.45) to evaluate the percentage of blue area in the Masson-trichrome section [22].

Evaluation of apoptosis

Apoptosis was determined by terminal deoxyribonucleotidyl transferase (TdT)-mediated biotin-16-deoxyuridine triphosphate (dUTP) nick-end labeling (TUNEL) staining using the Apoptosis *in situ* Detection Kit (#293–71501; Wako, Osaka, Japan). TUNEL-positive nuclei per field of view were manually counted in six sections of three groups (Control, DOB and CB) over a microscopic field of 20 x, averaged and expressed as the ratio of TUNEL-positive nuclei (%) [22,32]. Limiting the counting of total nuclei and TUNEL-positive nuclei to areas with a true cross section of myocytes made it possible to selectively count only those nuclei that were clearly located within myocytes. For some samples, TUNEL staining was performed using the In Situ Cell Death Detection Kit, Fluorescein (#11684795910; Sigma) with simultaneous immunostaining of dystrophin for muscle membrane identification and Hoechst staining for visualization of nuclei; the results confirmed that apoptotic cells identified and counted as TUNEL-positive nuclei by light microscopy were located inside the myofibers.

Evaluation of the number of microvessels per masseter myocyte

Frozen cross sections of the masseter muscle were immunohistochemically double-stained with antibodies against dystrophin (#D8168, Sigma) and CD31 (#ab28365, Abcam, Cambridge, UK). The number of microvessels per masseter myocyte was calculated as described previously [22,36].

Skinned muscle strand preparation and measurements of isometric force and ATPase activity

Muscle strands (5 mm long, 2 mm wide and 2 mm thick) were excised from the masseter muscle and skinned muscle strands were prepared as reported [37,38]. Isometric force and ATPase activity were measured in the relaxing solution (pCa 8.0) and the activating solutions with the various Ca^{2+} concentrations (pCa 6.1, 5.8, 5.5, 4.6) as described previously [37,38]. Results were analyzed and compared using Microsoft Excel 2010 (Microsoft Corporation, Redmond, WA, USA) and Igor Pro 3.15 (HULINKS Inc., Tokyo, Japan).

Western blotting

The excised right masseter muscle was homogenized in a Polytron (Kinematica AG, Lucerne, Switzerland) in ice-cold RIPA buffer (Thermo Fisher Scientific, Waltham, MA, USA: 25mM Tris-HCl (pH 7.6), 150mM NaCl, 1% NP-40, 1% sodium deoxycholate, 0.1% SDS) without addition of inhibitors [39], and the homogenate was centrifuged at 13,000 x *g* for 10 min at 4˚C. The supernatant was collected and the protein concentration was measured using a DC protein assay kit (Bio-Rad, Hercules, CA, USA). Equal amounts of protein (5 μg) were subjected to 12.5% SDS-polyacrylamide gel electrophoresis and blotted onto 0.2 mm PVDF membrane (Millipore, Billerica, MA, USA).

Western blotting was conducted with commercially available antibodies [22,32,40,41]. The primary antibodies against Akt (#9272), phospho-Akt (Ser-473, #9721), CaMKII (#3362), phospho-CaMKII (Thr-286, #3361), p44/42 MAPK (ERK1/2) (#4695), phospho-ERK1/2 (Thr-202/Tyr-204, #4370), BAX (#2772), microtubule-associated protein light chain 3 (LC3; #12741), mTOR (#2972), phospho-mTOR (Ser-2448, #5536; Ser-2481, #2974) and $β_1$-AR (#12271) were purchased from Cell Signaling Technology (Boston, MA, USA), the primary antibodies against GAPDH (sc-25778) and $β_2$-AR (sc-569) were purchased from Santa Cruz Biotechnology (Santa Cruz, CA, USA), the primary antibody against μ-calpain was purchased from Sigma, and the primary antibodies against phospholamban (PLN) (#A010-14) and phospho-PLN (Ser-16, #A010-12; Thr-17, #A010-13) were purchased from Badrilla (Leeds, UK). Horseradish peroxide-conjugated anti-rabbit or anti-mouse IgG (#NA934; GB Healthcare, Piscataway, NJ, USA) was used as a secondary antibody. The primary and secondary antibodies were diluted in Tris-buffered saline (pH 7.6) with 0.1% Tween 20 and 5% bovine serum albumin. The blots were visualized with enhanced chemiluminescence solution (ECL Prime Western Blotting Detection Reagent, GE Healthcare) and scanned with a densitometer (LAS-1000, Fuji Photo Film, Tokyo, Japan).

Cell culture and evaluation of apoptosis

Murine myoblast C2C12 cells were maintained as described previously [42]. In brief, cells were cultured in Dulbecco's modified Eagle's medium (DMEM; Fisher Scientific, Loughborough, UK) supplemented with 10% fetal bovine serum (FBS; Fisher Scientific, Loughborough, UK), 100 U/ml penicillin (Fisher Scientific, Loughborough, UK), and 100 U/ml streptomycin (Fisher Scientific) at 37˚C in 5% CO_2 and 95% air at 100% humidity. For the induction of differentiation, confluent cells were cultured in DMEM supplemented with 2% horse serum (Fisher Scientific; differentiation medium) and the antibiotics mentioned above for 4 days.

To examine subtype-specific apoptosis, DOB ($β_1$ agonist) or CB ($β_2$ agonist) was diluted in differentiation medium and added to the differentiated C2C12 myotubes at 10^{-4} M. The myotubes were further cultured for 24 hr and stained with propidium iodide (PI; DOJINDO, Kumamoto, Japan) together with immunohistochemistry with an anti-myosin heavy chain

antibody for detection of myosin and Hoechst staining for detection of nuclei [43]. We performed preliminary experiments in the concentration range of 10^{-4}–10^{-6} M, with reference to the previous study, and determined that 10^{-4} M was the optimal concentration for both DOB and CB [44].

Statistical analysis

All data are reported as mean ± SEM. Comparison of data was performed using ANOVA followed by Tukey's post test. Differences were considered significant when $P < 0.05$.

Results

Effects of DOB and CB on body weight and consumption of food and water

We monitored the daily consumption of pellet food (S1A Fig) and water (S1B Fig), and confirmed that there were no significant differences among the three groups (food: DOB ($n = 13$): 4.0 ± 0.2 g, CB ($n = 12$): 3.0 ± 0.4 g, Control ($n = 10$): 3.6 ± 0.2 g, P = NS (not significant) for DOB or CB vs. Control; water: DOB ($n = 13$): 7.3 ± 0.3 mL, CB ($n = 12$): 5.6 ± 0.7 mL, Control ($n = 10$): 6.3 ± 0.1 mL, P = NS for DOB or CB vs. Control). Body weight also showed no difference among the three groups before (Control (26 ± 0.5 mg), DOB (25 ± 0.6 mg) and CB (25 ± 0.7 mg)) and after the 1-week treatment period (Control (26 ± 0.5 mg), DOB (26 ± 0.6 mg) and CB (27 ± 0.6 mg)) [45] ($n = 6$ in each group, P = NS for DOB or CB vs. Control (0 day)) (S1C Fig).

Masseter muscle mass was significantly increased by CB but not by DOB

We next evaluated cardiac and masseter muscle hypertrophy in terms of muscle mass (S1D Fig and S1E Fig) and the muscle mass per tibia length ratio (mg/mm) (Fig 1B and 1C). In cardiac muscle, cardiac muscle mass and the cardiac muscle mass to tibial length ratio were significantly increased in the DOB group (cardiac muscle mass: Control ($n = 10$) vs. DOB ($n = 10$): 127 ± 3.3 vs. 172 ± 9.6 mg, $P < 0.01$; cardiac muscle mass/tibial lengh ratio: Control ($n = 10$) vs. DOB ($n = 13$): 6.7 ± 0.3 vs. 8.1 ± 0.4 mg/mm, $P < 0.01$), as well as in the CB group (cardiac muscle mass: Control ($n = 10$) vs. DOB ($n = 10$): 127 ± 3.3 vs. 162 ± 10.5 mg, $P < 0.01$; cardiac muscle mass/tibial length ratio: Control ($n = 10$) vs. CB ($n = 12$): 6.7 ± 0.3 vs. 7.8 ± 0.2, $P < 0.05$) (S1D Fig and S1B Fig). There was no significant difference between the two agonists, in agreement with reported findings [46]. However, in masseter muscle, the ratio was significantly increased in the CB group (masseter muscle mass: Control ($n = 10$) vs. CB ($n = 10$): 114 ± 2.9 vs. 168 ± 4.0 mg, $P < 0.01$; masseter muscle mass/tibial length ratio: Control ($n = 10$) vs. CB ($n = 12$): 5.7 ± 0.2 vs. 7.3 ± 0.4 mg/mm, $P < 0.05$), but not in the DOB group (masseter muscle mass: Control ($n = 10$) vs. DOB ($n = 10$): 114 ± 2.9 mg vs. 115 ± 2.6 mg, P = NS; masseter muscle mass/tibial length ratio: Control ($n = 10$) vs. DOB ($n = 13$): 5.7 ± 0.2 vs. 6.3 ± 0.3 mg/mm, P = NS) (S1E Fig and S1C Fig).

Next, to confirm the difference between the effects of DOB and CB in masseter muscle, we performed HE staining of masseter muscle and measured the fiber CSA (Fig 1D). The CSA was significantly increased in the CB group (Control ($n = 6$) vs. CB ($n = 5$): 1525 ± 149 vs. 2060 ± 72 μm^2, $P < 0.01$), but not in the DOB group (Control ($n = 6$) vs. DOB ($n = 6$): 1525 ± 149 vs. 1494 ± 69 μm^2, P = NS) (Fig 1D).

These data indicate that masseter muscle hypertrophy was mediated through the activation of β_2-AR, but not β_1-AR, whereas cardiac hypertrophy was mediated through the activation of both β_2-AR and β_1-AR.
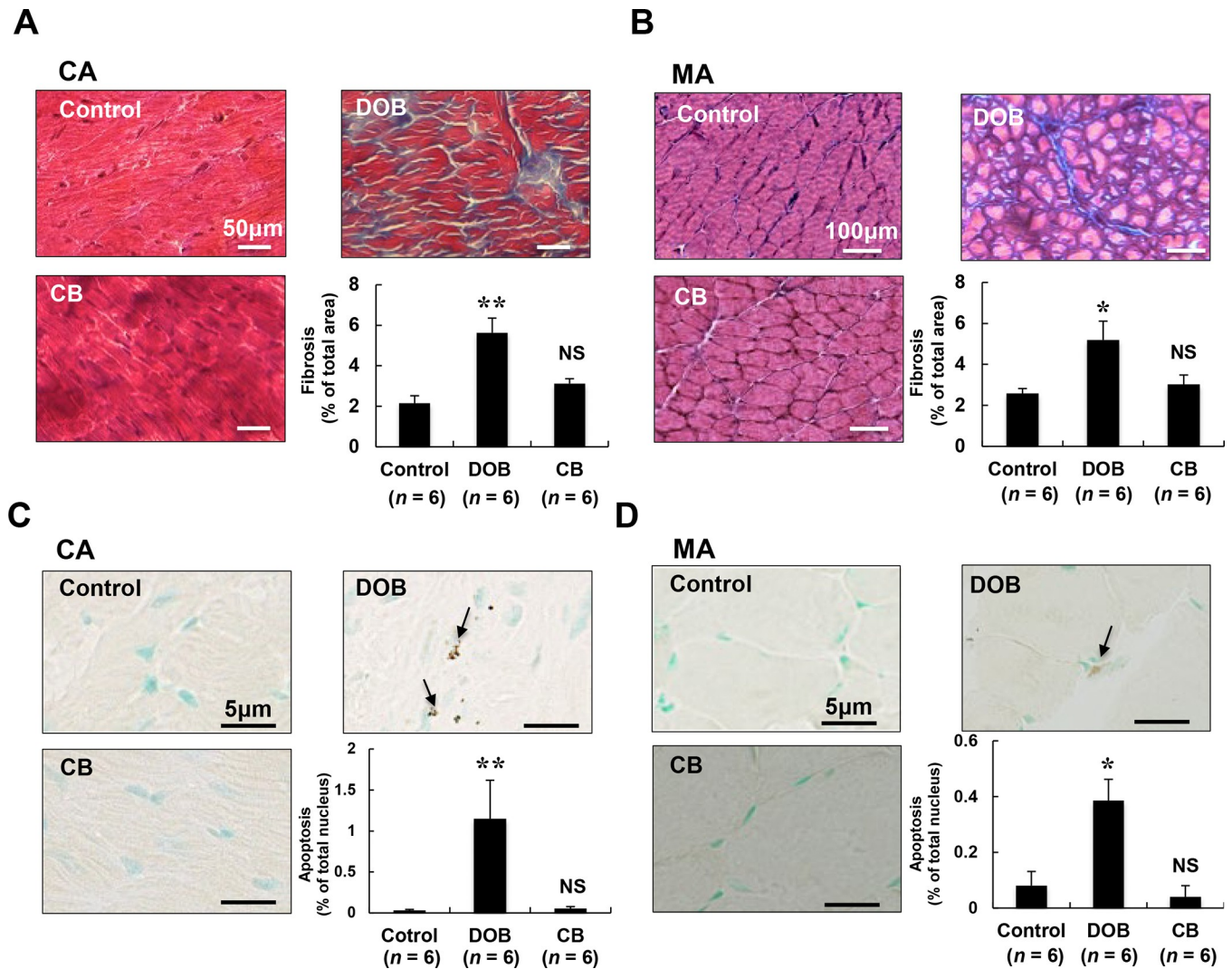
Fig 2. Effects of DOB and CB on fibrosis and apoptosis in cardiac and masseter muscles. (A-B) Representative images of Masson-trichrome-stained sections of cardiac muscle **(A)** and masseter muscle **(B)** in the Control (*upper left*), DOB (*upper right*) and CB (*lower left*) groups. The area of fibrosis was significantly increased in both the DOB-treated cardiac **(A)** and masseter **(B)** muscle (*$P < 0.05$, **$P < 0.01$ vs. Control), but not in the CB-treated cardiac **(A)** or masseter **(B)** muscle (*lower right*). Scale bars: 50 µm **(A)** and 100 µm **(B)**. **(C-D)** Representative images of TUNEL-stained sections of cardiac muscle **(C)** and masseter muscle **(D)** in the Control (*upper left*), DOB (*upper right*) and CB (*lower left*) groups. TUNEL-positive nuclei (black arrows) were counted in cardiac muscle **(C)** and masseter muscle **(D)** after 1 week of DOB or CB infusion and expressed as percentage of total myocytes (*lower right*). The number of TUNEL-positive nuclei was significantly increased in both the DOB-treated cardiac muscle (**$P < 0.01$ vs. Control) and masseter muscle (*$P < 0.05$ vs. Control), but not in the CB-treated cardiac or masseter muscle. Scale bars: 5 µm **(C)** and **(D)**. CA; cardiac muscle, MA; masseter muscle.

https://doi.org/10.1371/journal.pone.0215539.g002

Fibrosis was similarly and significantly increased by DOB in both cardiac and masseter muscles

We next examined the effects of chronic DOB or CB infusion on fibrosis in cardiac and masseter muscles by means of Masson-trichrome staining (**Fig 2A and 2B**). DOB significantly increased the area of fibrosis in cardiac (**Fig 2A**) and masseter muscles (**Fig 2B**) (cardiac muscle: Control ($n = 6$) vs. DOB ($n = 6$): 2.2 ± 0.4% vs. 5.6 ± 0.7%, $P < 0.01$; masseter muscle: Control ($n = 6$) vs. DOB ($n = 6$): 2.6 ± 0.2% vs. 5.2 ± 0.9%, $P < 0.05$). However, CB did not alter the area of fibrosis in cardiac muscle or masseter muscle (cardiac muscle: Control ($n = 6$) vs. CB

($n = 6$): 2.2 ± 0.4% vs. 3.1 ± 0.2%, P = NS; masseter muscle: Control ($n = 6$) vs. CB ($n = 6$): 2.6 ± 0.2% vs. 3.0 ± 0.5%, P = NS).

These data indicate that fibrosis in cardiac and masseter muscles is mediated through the activation of β_1-AR, but not β_2-AR.

Effects of CB and DOB in other muscles

We examined the effects of DOB on other skeletal muscles, TA (fast-twitch) and SOL (slow-twitch), by measuring the muscle mass per tibia length ratio. We also performed HE staining and compared the results with those derived from the masseter muscle (fast-twitch) (**S2A Fig and S2B Fig**). The TA muscle mass per tibia length ratio was not different between the Control and DOB group, but it was significantly greater in the CB group than that in the Control, as in the case of masseter muscle. Also, the area of fibrosis was greater in the DOB group than in the CB group, as in the case of masseter muscle (**S2A Fig**). Conversely, the SOL muscle mass per tibial length ratio was similar among the Control, DOB and CB groups, and no abnormal organization, such as fibrosis or muscle rupture, was observed (**S2B Fig**). Importantly, these results are consistent with the idea that activation of β_1-AR-mediated cAMP signaling with DOB might induce abnormality in fast-twitch muscle, but not in slow-twitch muscle, probably due to increased PDE4-mediated cAMP hydrolysis in SOL compared to masseter muscle or TA, resulting in a reduced cAMP concentration to activate the downstream β_1-AR-mediated cAMP signaling [12].

Myocyte apoptosis was similarly and significantly increased by DOB in both cardiac and masseter muscles

We also examined the effects of DOB and CB on myocyte apoptosis in cardiac (**Fig 2C**) and masseter muscles (**Fig 2D**) by means of TUNEL staining. Myocyte apoptosis in cardiac and masseter muscles was significantly increased by DOB (cardiac muscle: Control ($n = 6$) vs. DOB ($n = 6$): 0.03 ± 0.01 vs. 1.2 ± 0.5%, $P < 0.01$; masseter muscle: Control ($n = 6$) vs. DOB ($n = 6$): 0.01 ± 0.05 vs. 0.4 ± 0.08%, $P < 0.05$), whereas CB had no effect (cardiac muscle: Control ($n = 6$) vs. CB ($n = 6$): 0.03 ± 0.01 vs. 0.05 ± 0.02%, P = NS; masseter muscle: Control ($n = 6$) vs. DOB ($n = 6$): 0.08 ± 0.05 vs. 0.04 ± 0.04%, P = NS) (**Fig 2C and 2D**).

For some samples, we performed TUNEL staining (green) with simultaneous detection of dystrophin with antibody (red) for muscle membrane identification and visualization of nuclei with Hoechst (blue) by using confocal microscopy, and confirmed that apoptotic cells identified as TUNEL-positive nuclei by light microscopy were located inside the myofibers (**S2C Fig**).

These results, together with Masson-trichrome staining (**Fig 2A and 2B**), indicate that fibrosis and apoptosis in both cardiac and masseter muscles are mediated through the activation of β_1-AR, but not β_2-AR.

Apoptosis was significantly increased in C2C12 cells by DOB

We examined the effects of DOB and CB on apoptosis using differentiated murine myoblast C2C12 cells in vitro [44]. For the induction of myotube differentiation, cells were cultured in DMEM supplemented with 2% horse serum. We first examined the expression of β_1- and β_2-ARs by western blotting and confirmed that both expressions reached maximum at 5 days (Day 5) after the induction of cell differentiation (**S3A Fig**).

We thus treated C2C12 cells with DOB or CB at 10^{-4} M on Day 4, incubated them for 24 hr, and then (Day 5) performed PI staining with immunohistochemistry for simultaneous detection of myosin with an anti-myosin heavy chain antibody (green) and Hoechst staining

(blue) for visualization of nuclei (**S4A–S4C Fig**) [43]. PI-positive cells, which were also stained with an anti-myosin heavy chain antibody, were significantly increased by the DOB treatment (Control ($n = 3$) vs. DOB ($n = 3$): 2.2 ± 0.8 vs. 16.5 ± 1.2, $P < 0.01$), but not by the CB treatment (Control ($n = 3$) vs. CB ($n = 3$): 2.2 ± 0.8 vs. 4.4 ± 0.1, P = NS) (**S4D Fig**).

We also examined the expression of cleaved caspase-8, an apoptosis-related cysteine protease [47], and found that it was significantly increased by the DOB treatment (Control ($n = 4$) vs. DOB ($n = 6$); 100 ± 7.4 vs. 153 ± 13%, $P < 0.05$), but not by the CB treatment (Control ($n = 4$) vs. CB ($n = 6$); 100 ± 7.4 vs. 119 ± 14%, P = NS) (**S3B Fig**). These data were consistent with the in vivo studies shown in **Fig 2C and 2D**.

The number of microvessels per masseter myocyte was significantly decreased by DOB

Angiogenesis and hypertrophic response are closely associated in both skeletal muscle [48] and cardiac muscle [22,36]. We thus performed double immunostaining for dystrophin (red) and CD31 (green), and examined the number of microvessels per masseter myocyte in mice treated with DOB or CB (**S5A–S5C Fig**). There was no difference in the number of microvessels between the Control and CB group (Control ($n = 3$) vs. CB ($n = 3$): 4.5 ± 0.2 vs. 4.6 ± 0.3, P = NS). However, the number was significantly decreased in the DOB group (Control ($n = 3$) vs. DOB ($n = 3$): 4.5 ± 0.2 vs. 1.6 ± 0.2, $P < 0.01$) (**S5D Fig**).

These data suggest that activation of β_1-AR signaling might alter the number of microvessels in masseter muscle, and might also be associated with the blunted hypertrophic response of masseter muscle to the DOB treatment.

Ca²⁺ sensitivity of force and ATPase activity was not altered in DOB-treated mice

Cardiac as well as skeletal muscle function responds to a variety of changes in myocyte biology, including structural changes, altered Ca^{2+} handling, disrupted energetics, and modifications in myofibrillar function [49,50]. The Ca^{2+} sensitivity of force and ATP activity is regulated through the protein kinase A- or/and protein kinase C-mediated phosphorylation of myofilament protein in cardiac as well as skeletal muscle [51,52], but the effects of chronic β_1- or β_2-AR activation on calcium sensitivity in skeletal muscle have not been reported. We thus hypothesized that myofibrillar function might be altered in DOB-treated skinned masseter muscle.

As shown in **S6 Fig**, the Ca^{2+}-activated isometric force (*lower trace*) and the decrease of ATPase activity, measured in terms of the consumption rate of nicotinamide adenine dinucleotide (NADH) (*upper trace*) were simultaneously recorded in a skinned masseter muscle strands.

The curves representing the force-pCa relationship (**S7A Fig**) and the ATPase activity-pCa relationship (**S7B Fig**) in the Control, DOB and CB groups at the Ca^{2+} concentration of 6.1, 5.8, 5.5, 5.1 and 4.6 (expressed as pCa = -log [Ca^{2+}]) showed no leftward or rightward shift, suggesting that the Ca^{2+} sensitivity of force and ATPase activity were similar among the three groups. This might be due to the balance between the opposing effects of PKA (decrease of Ca^{2+} sensitivity; rightward shift) and Epac (increase of Ca^{2+} sensitivity; leftward shift) [53].

We also calculated the average pCa producing 50% force or ATPase activity, i.e., pCa_{50}, and the Hill coefficients, by fitting the data of Ca^{2+}-activated force and Ca^{2+}-activated ATPase activity within the pCa range from 6.1 to 4.6 for the three groups (**S7C Fig and S7D Fig**). Average pCa_{50} values (Ca^{2+} concentration required for half-maximal effect) of isometric force (**S7C Fig left**) and ATPase activity (**S7C Fig right**) were not significantly different among the three
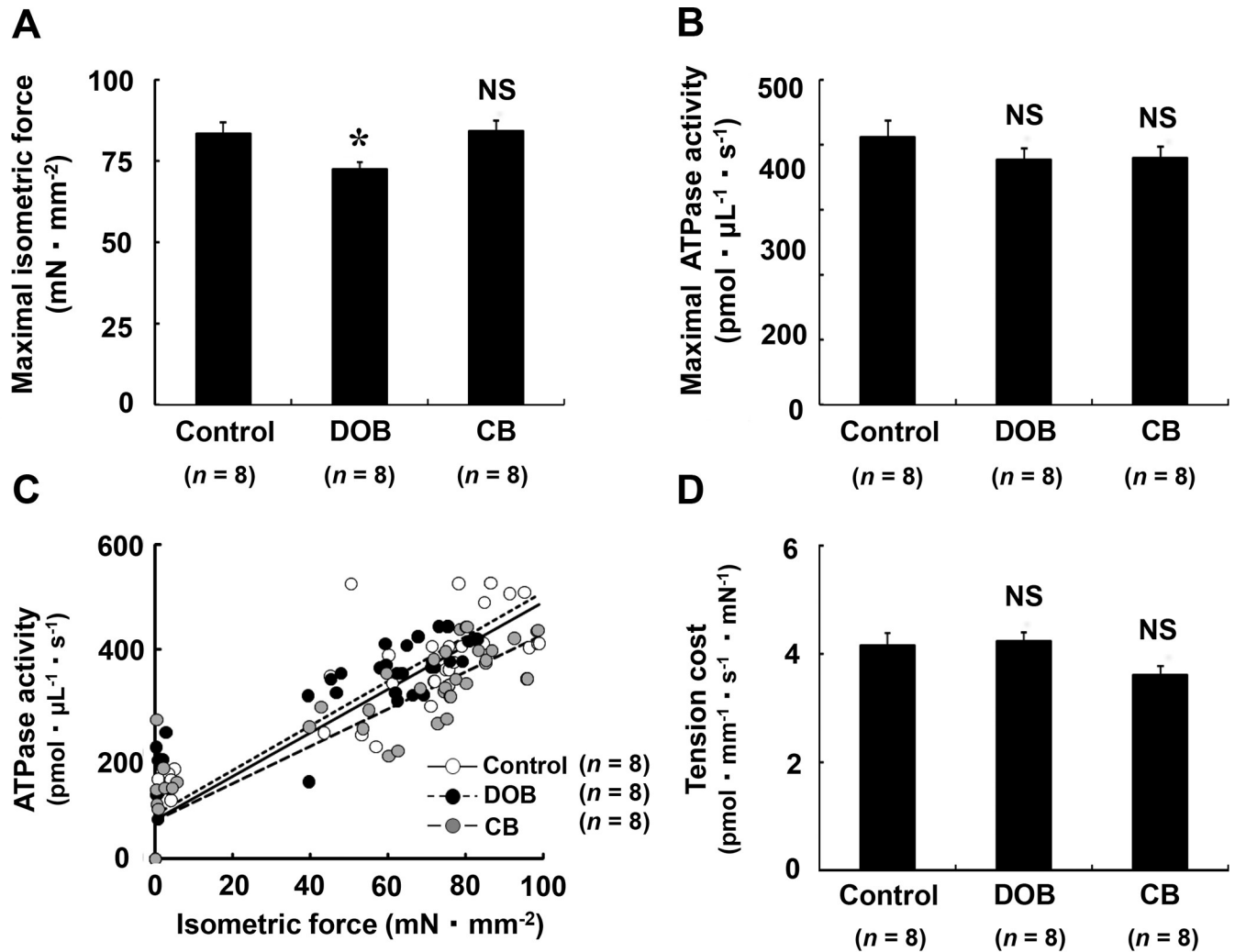
Fig 3. Effects of DOB and CB on maximal isometric force and ATPase activity and tension cost. (A) Maximal isometric force at pCa 4.6 (saturating $[Ca^{2+}]$) was significantly smaller in the DOB group than in the Control ($n = 8$ each). **(B)** Maximal ATPase activity at pCa 4.6 in the DOB group or the CB group showed no significant differences from the Control ($n = 8$ each). **(C)** Relationship between ATPase activity and isometric force in the skinned masseter preparations from the Control, DOB, and CB groups. The average ATPase activity values at pCa 6.1, 5.8, 5.5, 5.1 and 4.6 were plotted against the corresponding average force values. The data points of the three groups (open circle, Control; closed circle, DOB; gray circle, CB) were fitted by linear regression as indicated (solid line, Control; dashed line DOB; long dashed line CB). The formulae of the regression lines are y = 4.16x + 74.28, r = 0.91 (Control), y = 4.24x + 84.38, r = 0.91 (DOB), y = 3.56x + 73.37, r = 0.9 (CB), (r: correlation coefficient). Slopes of the regression lines (ATPase activity/isometric force) indicate the tension cost. **(D)** The average tension cost in the DOB group or the CB group showed no significant difference from the Control ($n = 8$ each). CA; cardiac muscle, MA; masseter muscle.

groups. Also, there were no significant differences of Hill coefficient (isometric force and ATPase activity) among the three groups (S7D Fig)

Maximal isometric force was decreased in DOB-treated mice

We next compared the isometric force and ATPase activity at the maximal level of Ca^{2+} activation (pCa = 4.6) in the Control, DOB and CB groups (Fig 3). Maximal isometric force was significantly smaller in the DOB group than in the Control (Control ($n = 8$) vs. DOB ($n = 8$): 84 ± 3.4 vs. 72 ± 2.3 mN/mm^2, $P < 0.05$), but no significant decrease was observed in CB mice (Control ($n = 8$) vs. CB ($n = 8$): 84 ± 3.4 vs. 84 ± 3.3 mN/mm^2, $P = $ NS) (Fig 3A). In marked

contrast, maximal ATPase activity was similar among the three groups (n = 8 each) (**Fig 3B**). In order to clarify the myofibrillar energy utilization in masseter muscle, we also examined the tension cost, i.e., ATPase activity/isometric force ratio, measured as the slope of the regression lines in the relationship between ATPase activity and isometric force (**Fig 3C**) and the values were similar among the three groups (n = 8 each) (**Fig 3D**).

Akt signaling was significantly increased by CB but not by DOB in both cardiac and masseter muscles

We then examined the phosphorylation of Akt in cardiac (**Fig 4A**) and masseter muscles (**Fig 4B**), since this is known to be involved in cell-protective [9,10] and hypertrophic pathways [54,55] in the heart.

Akt phosphorylation (Ser-473) of cardiac muscle was significantly increased in the CB group (Control (n = 6) vs. CB (n = 6): 100 ± 6.0 vs. 405 ± 99%, P < 0.05). Although it was also increased in the DOB group, this was not statistically significant (P = NS vs. Control, n = 6 each) (**Fig 4A**). Akt phosphorylation (Ser-473) of masseter muscle was also significantly increased in the CB group (Control (n = 6) vs. CB (n = 5): 100 ± 8.4 vs. 132 ± 7.9 mg P < 0.05), but not in the DOB group (Control (n = 6) vs. DOB (n = 6): 100 ± 8.4 vs. 96 ± 8.7 mg P = NS) (**Fig 4B**).

These data suggest that induction of hypertrophy by CB in both cardiac and masseter muscle might be mediated, at least in part, through the activation (phosphorylation at Ser-473) of Akt.

ERK1/2 activation was significantly increased by DOB but not by CB in both cardiac and masseter muscles

ERK1/2 activation is known to be involved in the development of cardiac fibrosis [56,57]. We thus examined the amount of phospho-ERK1/2 (Thr-202/Tyr-204) in cardiac (**Fig 4C**) and masseter muscles (**Fig 4D**) of DOB- or CB-treated mice. ERK1/2 phosphorylation (Thr-202/Tyr-204) in cardiac muscle was significantly increased in the DOB group (Control (n = 4) vs. DOB (n = 4): 100 ± 11 vs. 246 ± 63%, P < 0.05), but not in the CB group (Control (n = 4) vs. CB (n = 6): 100 ± 11 vs. 106 ± 19%, P = NS) (**Fig 4C**). ERK1/2 phosphorylation (Thr-202/Tyr-204) in masseter muscle was also significantly increased in the DOB group (Control (n = 6) vs. DOB (n = 6): 100 ± 31 vs. 329 ± 60%, P < 0.05), but not in the CB group (Control (n = 6) vs. CB (n = 6): 100 ± 31 vs. 149 ± 58%, P = NS) (**Fig 4D**).

These data suggest that DOB-mediated fibrosis in both cardiac and masseter muscle might be mediated, at least in part, through activation of ERK1/2 signaling.

BAX expression was significantly increased by DOB in both cardiac and masseter muscles

We also examined changes of BAX, an accelerator of apoptosis, in cardiac (**Fig 5A**) and masseter muscle (**Fig 5B**) and found that its expression was significantly increased by DOB (cardiac muscle: Control (n = 5) vs. DOB (n = 5): 100 ± 12 vs. 232 ± 102%, P < 0.05; masseter muscle: Control (n = 5) vs. DOB (n = 5): 100 ± 13 vs. 441 ± 117%, P < 0.05), but not by CB (P = NS for both cardiac and masseter muscles vs. Control).

Autophagy was induced by CB but not by DOB in cardiac and masseter muscles

We next investigated the effects of DOB and CB treatment on autophagy in the cardiac and masseter muscles, because autophagy is important to maintain muscle homeostasis
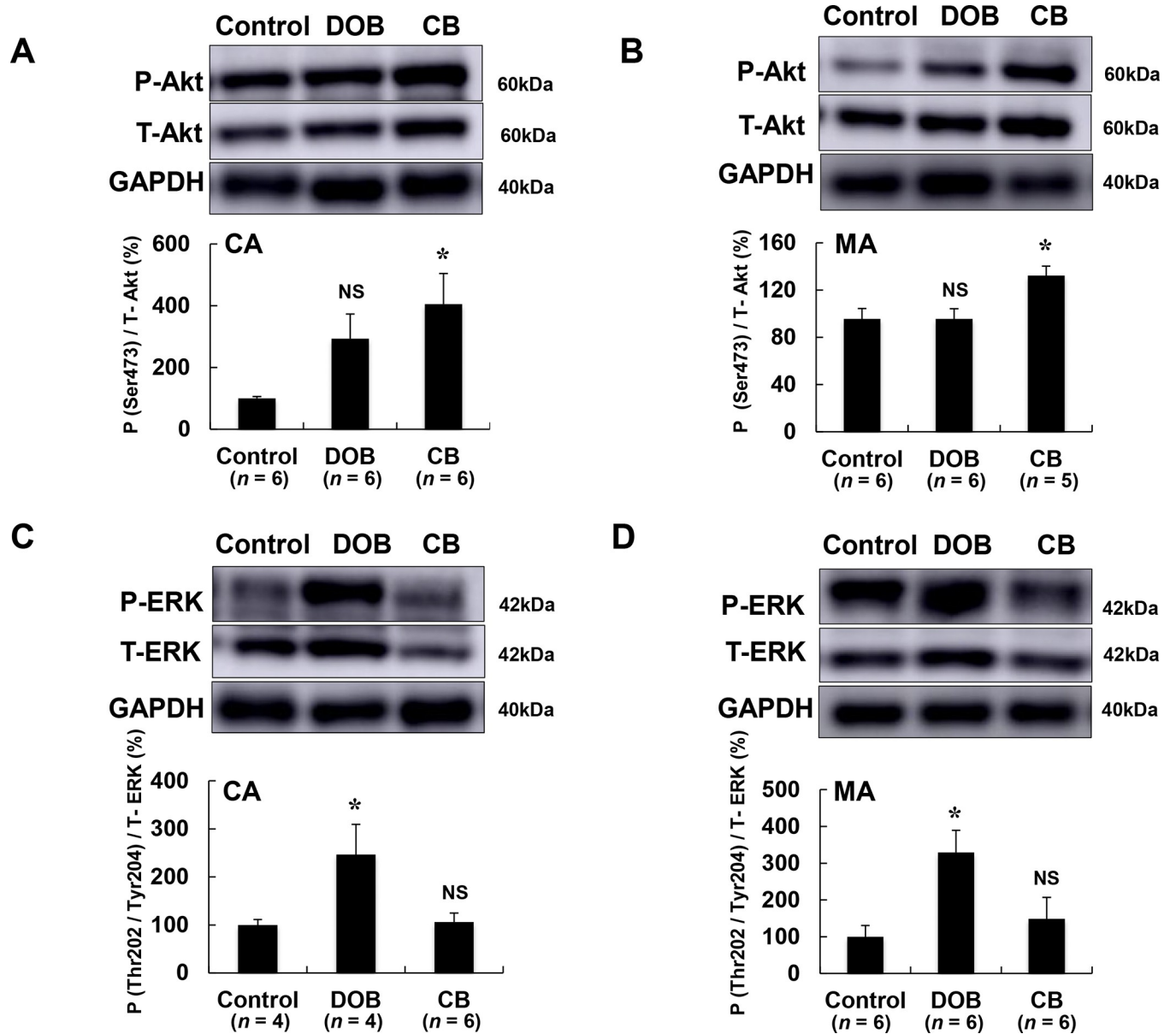
Fig 4. Effects of DOB and CB on Akt and ERK1/2 signaling pathways in cardiac and masseter muscles. (A) Akt phosphorylation (Ser-473) of cardiac muscle was significantly increased in the CB group ($^*P < 0.05$ vs. Control). It was also increased, though without statistical significance, in the DOB group. (B) Akt phosphorylation (Ser-473) of masseter muscle was significantly increased in the CB group ($^*P < 0.05$ vs. Control), but not in the DOB group. (C) ERK1/2 phosphorylation (Thr-202/Tyr-204) in cardiac muscle was significantly increased in the DOB group ($^*P < 0.05$ vs. Control), but not in the CB group. (D) ERK1/2 phosphorylation (Thr-202/Tyr-204) in masseter muscle was also significantly increased in the DOB group ($^*P < 0.05$ vs. Control), but not in the CB group. CA; cardiac muscle, MA; masseter muscle.

https://doi.org/10.1371/journal.pone.0215539.g004

physiologically and in response to stress [58]. Also, augmenting autophagy was reported to be protective [59], while suppressing autophagy was reported to be deleterious to the heart. We thus hypothesized that autophagy might be induced after β_2-AR stimulation with CB, but not after β_1-AR stimulation with DOB, in cardiac and skeletal muscle.

LC3-II, an autophagosome marker, was significantly increased in both cardiac (**Fig 5C**) and masseter muscles (**Fig 5D**) of the CB group (cardiac muscle: Control ($n = 6$) vs. CB ($n = 3$): 100 ± 12 vs. $176 \pm 24\%$, $P < 0.05$; masseter muscle: Control ($n = 4$) vs. CB ($n = 4$): 100 ± 9 vs.
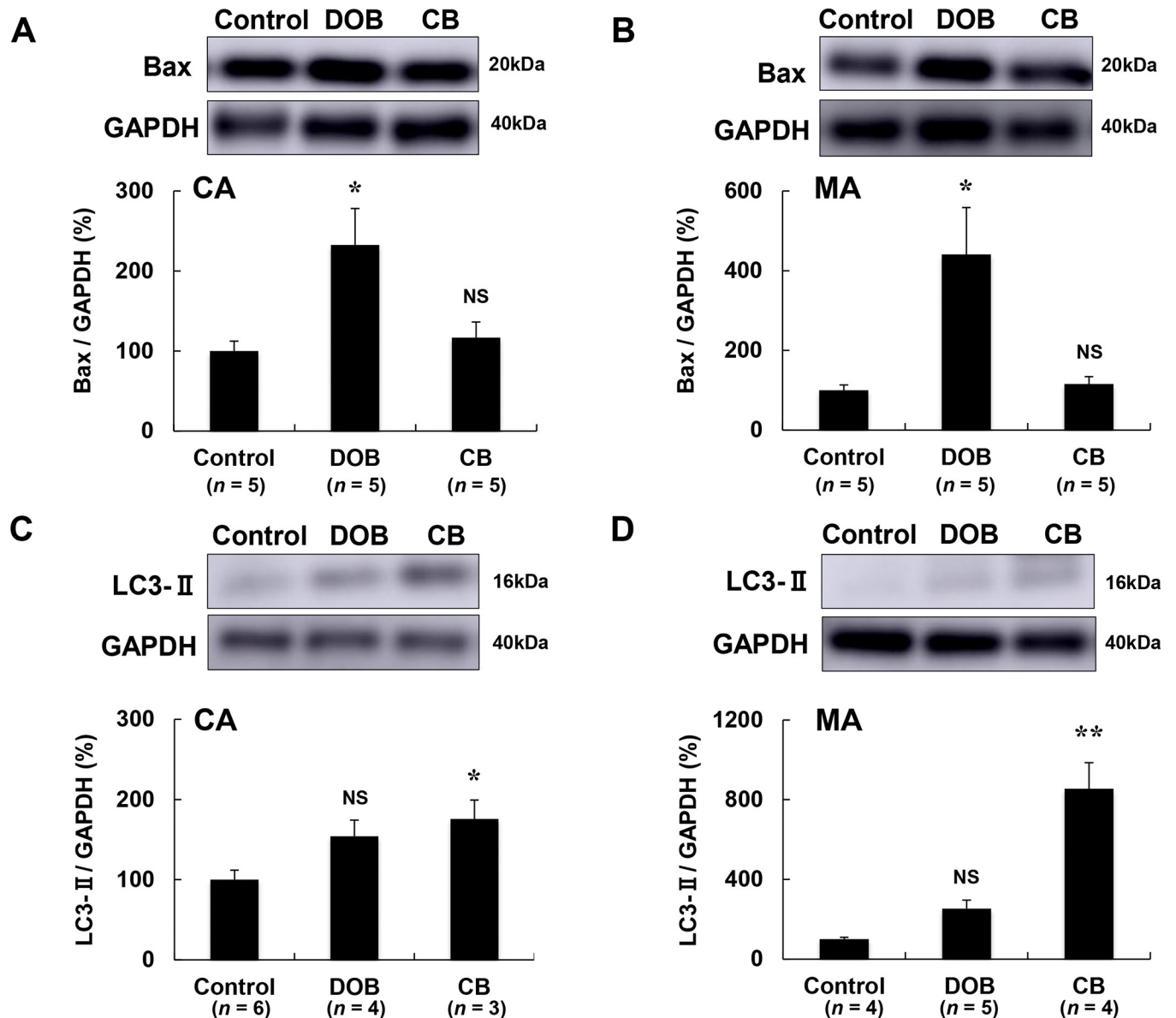
Fig 5. Effects of DOB and CB on expression of BAX and LC3 in cardiac and masseter muscles. **(A-B)** BAX expression was significantly increased in the DOB group, but not in the CB group, in both cardiac **(A)** and masseter **(B)** muscles ($*P < 0.05$ each vs. Control). **(C-D)** LC3-II expression was significantly increased in the CB group, but not in the DOB group, in both cardiac **(C)** and masseter muscles **(D)** ($*P < 0.05$ or $**P < 0.01$ each vs. Control). MA; masseter muscle.

$854 \pm 263\%$, $P < 0.01$). In contrast, LC3-II expression was not significantly increased in either cardiac (**Fig 5C**) or masseter (**Fig 5D**) muscle of the DOB group.

These data suggest that activation of autophagy might be induced efficiently by activation of β_2-AR rather than β_1-AR in both cardiac and masseter muscles [60,61].

mTORC1 was activated by CB and mTORC2 was activated by DOB in masseter muscle

mTOR phosphorylation at serine 2448 (mTORC1) is regulated by PI3-Akt signaling and mTOR phosphorylation at serine 2481 (mTORC2) is regulated by the cAMP-PKA pathway in

skeletal muscle [11,17]. Also, PI3-Akt signaling is known to be protective and cAMP-PKA signaling is deleterious for cardiac muscle [32,55]. We thus hypothesized that mTOR phosphorylation at serine 2448 (mTORC1) might be mediated by β_2-AR stimulation with CB and mTOR phosphorylation at serine 2481 (mTORC2) might be mediated by β_1-AR stimulation with DOB in masseter muscle.

We found that mTOR phosphorylation at serine 2448 was significantly increased in the CB group (Control ($n = 8$) vs. CB ($n = 8$): 100 ± 10 vs. $171 \pm 21\%$, $P < 0.01$) but not in the DOB group ($92 \pm 8.9\%$, $P = $ NS vs. Control, $n = 8$) (**Fig 6A**). Conversely, mTOR phosphorylation at serine 2481 was significantly increased in the DOB group (Control ($n = 8$) vs. DOB ($n = 8$): 100 ± 6 vs. $150 \pm 12\%$, $P < 0.05$) but not in the CB group ($118 \pm 13\%$, $P = $ NS vs. Control, $n = 8$) (**Fig 6B**).

These data suggest that masseter muscle fibrosis and apoptosis in DOB-treated mice might be associated with the activation of mTORC2 signaling.

CaMKII phosphorylation and oxidation were significantly increased by DOB in masseter muscle

CaMKII is crucial for cardiac excitation-contraction coupling and its expression is increased in heart failure in animals and humans [62,63]. However, the role of CaMKII in skeletal muscle has not yet been examined. Thus, we examined the effects of DOB or CB on CaMKII phosphorylation at threonine 286 and CaMKII oxidation in masseter muscle.

CaMKII phosphorylation (Thr-286) was significantly increased in the DOB group (Control ($n = 6$) vs. DOB ($n = 4$): 100 ± 39 vs. $450 \pm 74\%$, $P < 0.01$), but not in the CB group ($151 \pm 72\%$, $P = $ NS vs. Control) (**Fig 6C**). CaMKII oxidation was also significantly increased in the DOB group (Control ($n = 3$) vs. DOB ($n = 4$): 100 ± 9.6 vs. $255 \pm 60\%$, $P < 0.05$), but not in the CB group ($83 \pm 11\%$, $P = $ NS vs. Control) (**Fig 6D**).

These data suggest that masseter muscle fibrosis and apoptosis might be mediated, at least in part, through the activation of CaMKII signaling.

Ca^{2+} homeostasis was altered in DOB-treated mice

The maintenance of calcium (Ca^{2+}) homeostasis during muscle contraction is requisite for optimal contractile function, and altered Ca^{2+} homeostasis might induce hyperactivation of calcineurin-NFAT signaling and calpain signaling [64,65].

We assessed the levels of Ca^{2+}-handling proteins involved in Ca^{2+} homeostasis in skeletal muscle. We first examined the activation level of calcineurin-NFAT signaling in terms of phosphorylation level on serine 259 of NFATc1 [66], and found that it was significantly greater in masseter muscle of DOB mice than in control mice (Control ($n = 3$) vs. DOB ($n = 3$): 100 ± 40 vs. $570 \pm 84\%$, $P < 0.01$), whereas this was not the case in CB-treated mice (Control ($n = 3$) vs. CB ($n = 3$): 100 ± 40 vs. $333 \pm 24\%$, $P = $ NS) (**Fig 7A**).

Calpain is an intracellular Ca^{2+}-activated cysteine protease, but the physiological roles of calpains are not well understood, although μ-calpain has been associated with skeletal muscle remodeling [14]. Calpains are present predominantly in their full-length, unautolysed/unactivated forms at rest. However, calpain appears in autolysed forms upon activation and measurement of these forms can be used to determine when in vivo induction of Ca^{2+}-mishandling occurs in a Ca^{2+}-dependent manner [14]. We thus examined μ-calpain activity by measuring the autolysis level in masseter muscle and found that μ-calpain autolysis was significantly greater in masseter muscle of DOB mice than in the control group (Control ($n = 4$) vs. DOB ($n = 5$): 25 ± 0.8 vs. $32 \pm 1.2\%$, $P < 0.05$), whereas no significant increase was observed in CB mice (Control ($n = 4$) vs. CB ($n = 6$): 25 ± 0.8 vs. $23 \pm 1.5\%$, $P = $ NS) (**Fig 7B**).
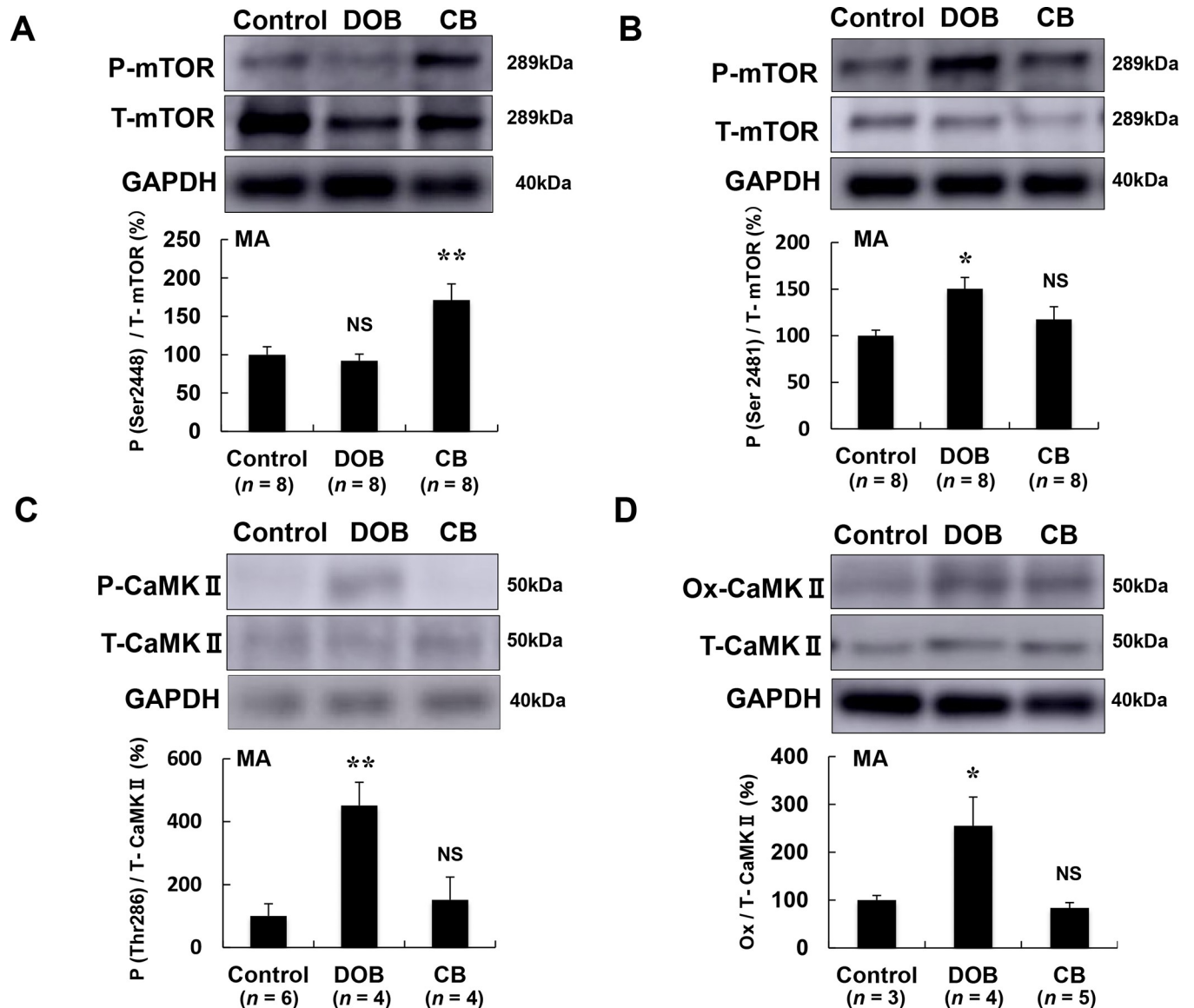
Fig 6. Effects of DOB and CB on mTORC1/C2 and CaMKII signaling pathways in masseter muscle. (A) In masseter muscle, mTOR phosphorylation on serine 2448, a specific marker of mTORC1 formation, was significantly increased in the CB group ($^{**}P < 0.01$ vs. Control), but not in the DOB group in masseter muscle. (B) mTOR phosphorylation on serine 2481, a specific marker of mTORC2 formation, was significantly increased in the DOB group ($^{*}P < 0.05$ vs. Control), but not in the CB group in masseter muscle. (C-D) CaMKII phosphorylation was significantly increased in the DOB group ($^{**}P < 0.01$ vs. Control), but not in the CB group (C). CaMKII oxidation was also significantly increased in the DOB group ($^{*}P < 0.05$ vs. Control), but not in the CB group (D). MA; masseter muscle.

https://doi.org/10.1371/journal.pone.0215539.g006

These data, together with the increased NFATc1 phosphorylation level in response to DOB treatment, indicated that calcium homeostasis was altered in masseter muscle of DOB-treated mice.

PLN phosphorylation was significantly increased by DOB in masseter muscle

The importance of PLN regulation of SERCA function in cardiac muscle health and disease is well established [22]. Recently, several studies have indicated that it might also play an important role in the development of skeletal muscle disease [24,25]. We thus examined the effects
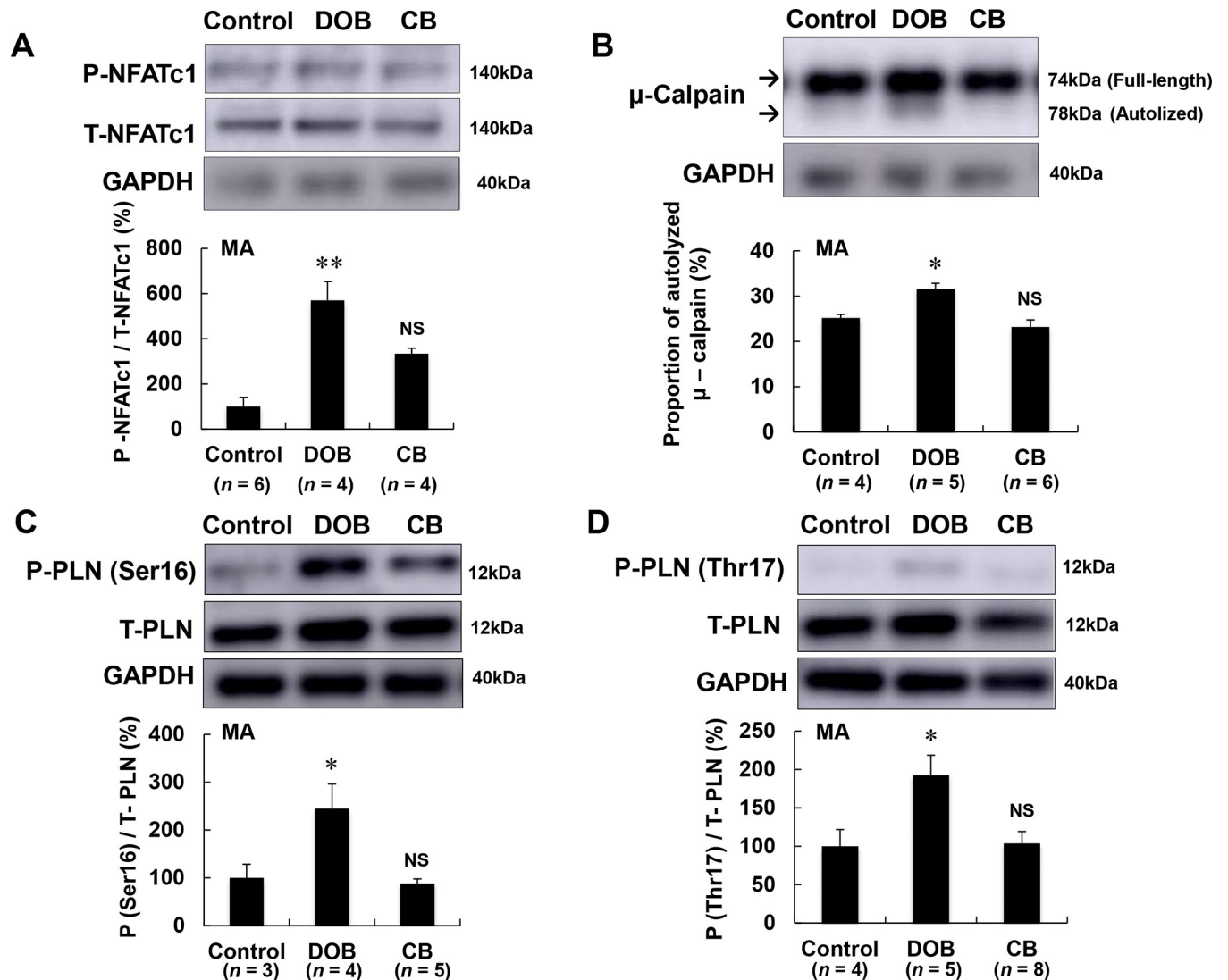
Fig 7. Effects of DOB and CB on Ca^{2+} homeostasis and PLN phosphorylation in masseter muscle. (A) NFATc1 phosphorylation on serine 259 was significantly greater in masseter muscle of the DOB group compared with the control group ($^*P < 0.05$ vs. Control), but this was not the case in the CB group. **(B)** The calculated μ-calpain fractional activation index (i.e., percentage of autolysed calpain) was significantly increased in the DOB group ($^{**}P < 0.01$ vs. Control), but not in the CB group. **(C)** PLN phosphorylation (Ser-16) was significantly increased in the DOB group ($^*P < 0.05$ vs. Control), but not in the CB group. **(D)** PLN phosphorylation (Thr-17) was significantly increased in the DOB group ($^*P < 0.05$ vs. Control), but not in the CB group.

of DOB and CB on PLN phosphorylation (Ser-16) (Fig 7C) and PLN phosphorylation (Thr-17) in masseter muscle (Fig 7D).

PLN phosphorylation (Ser-16) was significantly increased in the DOB group (Control ($n = 3$) vs. DOB ($n = 4$): 100 ± 28 vs. $245 \pm 52\%$, $P < 0.05$), but not in the CB group (Control ($n = 3$) vs. CB ($n = 5$): 100 ± 28 vs. $88 \pm 9\%$, $P =$ NS) (Fig 7A). We further examined the PLN phosphorylation at Thr-17 and found that it was also significantly increased in the DOB group (Control ($n = 4$) vs. DOB ($n = 5$): 100 ± 22 vs. $192 \pm 26\%$, $P < 0.05$), but not in the CB group (Control ($n = 4$) vs. CB ($n = 8$): 100 ± 22 vs. $104 \pm 15\%$, $P =$ NS) (Fig 7B).

These data suggest that DOB-mediated masseter muscle fibrosis (Fig 2B) and apoptosis (Fig 2D) might be induced, at least in part, through increased PLN phosphorylation at serine 16 and threonine 17, as we previously showed to be the case in cardiac muscle [22].

Discussion

In this study, we examined the effects of chronic β_1-AR or β_2-AR stimulation on cardiac and masseter muscles of mice, using a selective β_1-AR agonist (DOB) and a selective β_2-AR agonist (CB). We have demonstrated that activation of β_1-AR signaling plays an important role in the development of myocyte apoptosis and fibrosis not only in cardiac muscle, but also in skeletal muscle.

In this study, cardiac hypertrophy in terms of cardiac muscle mass/tibial length ratio was significantly increased by approximately 21% in the DOB group (2 mg/kg/day for 1 week) and by approximately 16% in the CB group (2 mg/kg/day for 1 week) (**Fig 1B**). In previous studies in mice, the non-specific β-AR agonist isoproterenol (30 mg/kg/day for 1 week) induced cardiac hypertrophy by approximately 17% [67], while the β_2-AR specific agonist CB (2 mg/kg/day for 4 weeks) also induced cardiac hypertrophy by approximately 17% [68], suggesting that hypertrophic response was similar to our study, even though the dose and treatment period were greater.

The cardiac hypertrophy found in this study, as well as in previous reports, suggest that the local tissue concentrations of DOB and CB used in this study would have been sufficient to activate β_1-AR and β_2-AR, respectively, in skeletal muscle, as well as in cardiac muscle. Thus, we think the experimental conditions used in this study might be appropriate to examine the role of β_1-AR and β_2-AR signaling of skeletal muscle in mice. So, we think the current findings in skeletal muscle exposed to β_1-AR stimulation with DOB (2 mg/kg/day for 1 week) or β_2-AR stimulation with CB (2 mg/kg/day for 1 week) properly reflect the roles of β_1-AR and β_2-AR signaling in skeletal muscle.

This study, together with previous studies, suggested that an endogenous β_1-selective agonist norepinephrine, which is markedly increased in heart failure patients, induces deterioration of contractility of not only cardiac muscle [69,70], but also fast-twitch skeletal muscles such as masseter and TA muscles. On the other hand, β_2-AR signaling is protective via the increase of muscle hypertrophy and contractility and the decrease of myocardial apoptosis not only in cardiac muscle, but also in skeletal muscle [71], indicating that β_1-AR-mediated cAMP signaling in cardiac and fast-twitch skeletal muscle might play important roles in the induction of muscle dysfunction independently of their expression levels in each muscle, as demonstrated previously in TA and SOL [12].

Both β_1-AR and β_2-AR stimulate the classic Gsα-adenylyl cyclase-cAMP signaling cascade, but β_2-AR couples to both Gsα and Giα proteins, activating bifurcated signaling pathways (**Fig 8**). In the cardiac muscle, chronic β_1-AR stimulation with DOB induced cardiac remodeling (hypertrophy, fibrosis and myocyte apoptosis) together with increased BAX expression and ERK1/2 phosphorylation (Thr-202/Tyr-204); this is known to be a reactive oxygen species (ROS)-mediated pathway resulting in cardiac injury [72,73]. On the other hand, chronic β_2-AR stimulation with CB induced cardiac hypertrophy together with activation of Akt (Ser-473), which is a powerful promoter of cell survival and physiological hypertrophy [55,74].

In contrast to the cardiac muscle, chronic β_1-AR stimulation with DOB did not induce hypertrophy of masseter muscle, but caused muscle fibrosis and myocyte apoptosis with increased BAX expression, ERK1/2 phosphorylation (Thr-202/Tyr-204) and CaMKII phosphorylation (Thr-286) (**Fig 8**), though Akt phosphorylation (Ser-473) was not induced. On the other hand, chronic β_2-AR stimulation with CB induced masseter muscle hypertrophy with activation of Akt (Ser-473), but did not induce myocyte apoptosis or fibrosis. We also identified a significant increase of LC3-II protein expression, an autophagosome marker, in masseter muscle of CB-treated mice, but not DOB-treated mice. Proper regulation of the autophagy flux is critical for skeletal muscle homeostasis in response to various stresses and physiological
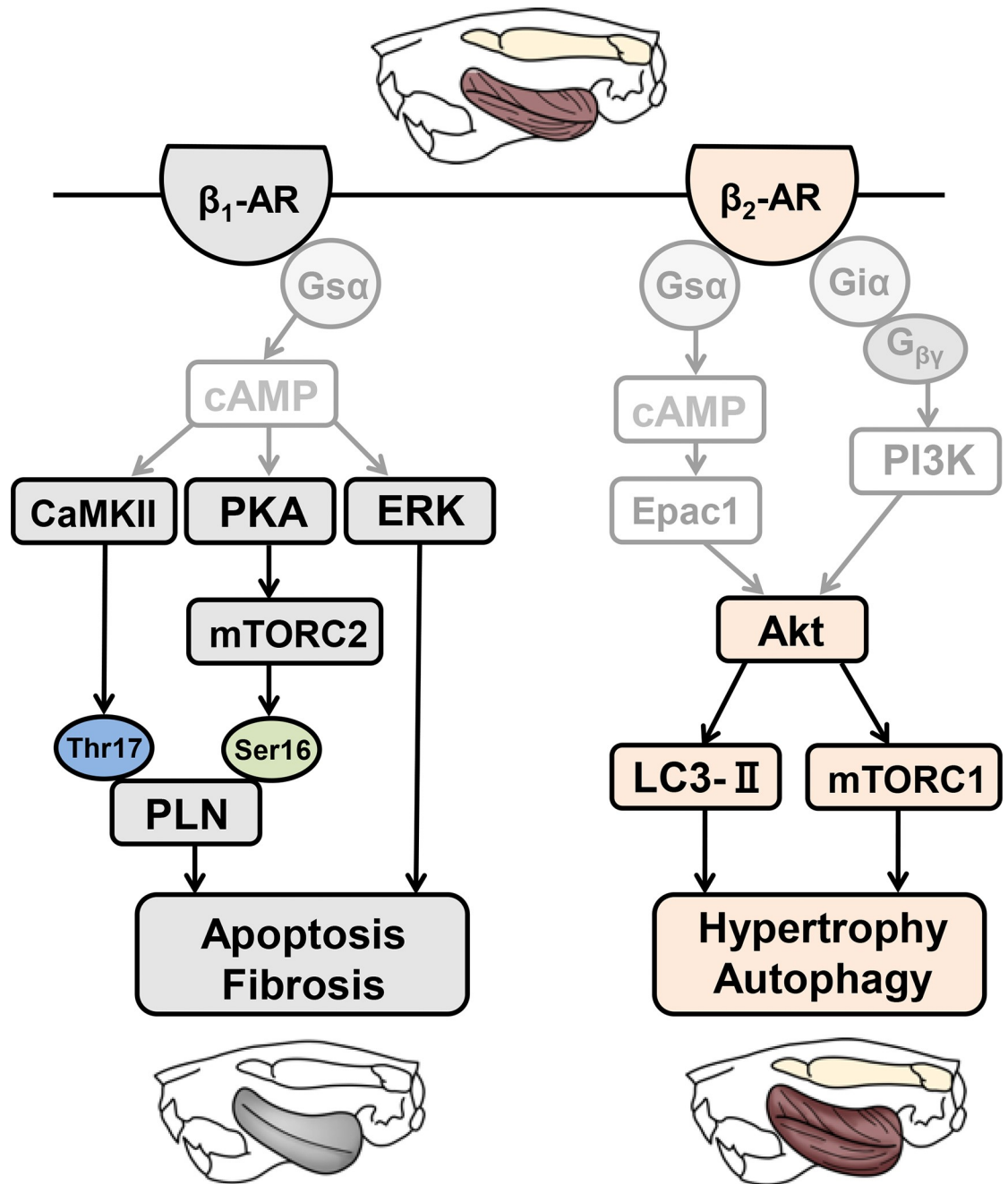
Fig 8. Schematic illustration of the proposed roles of β-AR signaling in masseter muscle. This scheme illustrates the proposed relationship of β_1-AR and β_2-AR signaling in masseter muscle. Chronic β_1-AR stimulation with DOB induces muscle fibrosis and apoptosis with the increase of ERK1/2, CaMKII and mTORC2 activation (*left*). Chronic β_1-AR stimulation with CB induces muscle hypertrophy and autophagy with increase of mTORC1 activation and LC3-II expression (*right*). Solid black lines represent findings in this study and solid grey lines represents findings reported previously (Lynch et al., 2008 [93], Ohnuki et al. 2014 [11], Ohnuki et al 2016 [12], Okumura et al. 2014 [22]).

stimuli [58]. More recently, it has been suggested that β_2-AR signaling might contribute to exercise training-mediated adaptations in insulin signaling and autophagy regulation through peroxisome-proliferator-activated receptor-γ coactivator-1α in skeletal muscle [75]. Taken

together, these results indicate that β_2-AR may be beneficial by promoting muscle hypertrophy and autophagy might be beneficial in response to various stresses (**Fig 8**).

In order to examine the reason for the different effects of β_1-AR stimulation in masseter muscle and cardiac muscle, we focused on mTOR, which is a downstream target of Akt and ERK1/2, and integrates a variety of environmental cues to regulate organismal growth and homeostasis [76]. mTOR assembles into two distinct multiprotein complexes, termed mTOR complex 1 (mTORC1) and mTORC2: it is phosphorylated at serine 2448 within the mTORC1 complex (associated with Raptor; regulatory associated protein of mTOR) and at serine 2481 within the mTORC2 complex (associated with Rictor; rapamycin insensitive companion of mTOR) [77]. It was recently shown that mTOR phosphorylation at serine 2448 (mTORC1) is regulated by PI3K-Akt signaling, while mTOR phosphorylation at serine 2481 (mTORC2) is regulated by the cAMP-PKA pathway in skeletal muscle [17].

In this study, mTOR phosphorylation (Ser-2448) was significantly increased by CB but not by DOB, while mTOR phosphorylation (Ser-2481) was significantly increased by DOB but not by CB. The experimental data in this study is consistent with the previous finding that mTORC1 signaling might regulate cell growth and proliferation in response to insulin, nutrients, and growth factors [17,76]. In contrast, much less is known about the role of mTORC2. Insofar as sympathetic tone increases with age, our data might indicate that activation of mTORC2 plays a pivotal role in the development of skeletal muscle weakness through the accumulation of skeletal muscle apoptosis and fibrosis induced via β_1-AR stimulation during aging.

PLN is a well-known inhibitor of SERCA2a that maintain low levels of cytosolic Ca^{2+} in muscle and play a crucial role in muscle contraction [21]. The importance of PLN regulation of SERCA2a function in cardiac muscle health and disease is well established [78,79]. Indeed, decreased PLN phosphorylation, leading to a decrease of Ca^{2+} uptake by SERCA2a, is a central feature of heart failure [80,81], and decreased inhibition of SERCA2a by PLN ablation can prevent progression of heart failure [82,83]. Conversely, other groups found that decreased inhibition of SERCA2a through increased PLN phosphorylation might exaggerate heart failure and arrhythmogenic activity [84,85]. More recently, we have demonstrated that disruption of Epac1 protects the heart from chronic catecholamine stress, chronic pressure overload, and arrhythmogenic susceptibility through the inhibition of PLN phosphorylation (Ser-16 and Thr-17), together with decreased RyR2 phosphorylation (Ser-2808 and Ser-2814) [22]. However, the role of PLN phosphorylation in the development of skeletal muscle diseases remains poorly understood.

In this study, we found that chronic β_1-AR stimulation did not induce muscle hypertrophy in masseter muscle, but it caused muscle fibrosis and apoptosis with an increase of PLN phosphorylation (Ser-16 and Thr-17), indicating that increase of β_1-AR-mediated PLN phosphorylation might alter the Ca^{2+} leakage from sarcoplastic reticulum in skeletal muscle, as in the case in cardiac muscle [22].

Mouse and rabbit models overexpressing PLN in slow-twitch muscle fibers (PLN-TG) have been generated by attaching a PLN transgene to the β-myosin heavy chain promoter, which preferentially directs high levels of expression of slow-twitch muscle specific transgene. Importantly, PLN-TG mice show muscular dystrophy, including severe muscle wasting, fibrosis, fatty infiltration and muscle weakness [24,25].

β_2-AR stimulation has been reported to evoke vasodilatation in skeletal muscle, including masseter muscle, and impaired β_2-AR function is implicated in the maintenance of systemic arterial hypertension [86,87]. β_2-AR-mediated vasodilatation is caused through the upregulation of endothelial nitric oxide synthase via the PI3-kinase-Akt pathway in mouse pulmonary artery or rat cerebral artery [88,89]. More importantly, cardiorespiratory function and cerebral

blood oxygen influence cognitive function, physical performance, and rhythmic movement of the masseter muscle [90–92]. Also β_2-AR-gene deletion in mice leads to impaired insulin secretion by pancreatic β-cells, indicating that impaired β_2-AR function might alter insulin sensitivity and insulin signaling in skeletal muscle [27]. Thus, the β_2-AR-mediated protective effects in masseter muscle described in our current study, as well as in previous reports, might be mediated via not only through direct mechanisms involving β_2-AR in masseter muscle, but also in part via circulatory and/or hormonal indirect mechanisms.

As shown in **S2A Fig** and **S2B Fig**, we examined the effects of β_1-AR stimulation with DOB on the tissue morphology of TA (fast-twitch) and SOL (slow-twitch) in terms of the muscle mass per tibial length ratio and HE staining. We found that β_1-AR stimulation did not induce hypertrophy but induced fibrosis, as in the case of masseter muscle (fast-twitch muscle) [11,12]. These data suggest that activation of β_1- and β_2-AR signaling in **Fig 8** might be specific to fast-twitch muscles such as masseter and TA muscles.

Taken together with the previous findings, our results indicate for the first time that the β_1-AR signaling pathway is a potential therapeutic target for the treatment of skeletal muscle wasting and weakness.

Supporting information

S1 Fig. S1 Fig PLOS ONE-3rd revised.pdf. and S1 Fig.
(PDF)

S2 Fig. S2 Fig PLOS ONE-3rd revised.pdf and S2 Fig.
(PDF)

S3 Fig. S3 Fig PLOS ONE-3rd revised.pdf and S3 Fig.
(PDF)

S4 Fig. S4 Fig PLOS ONE-3rd revised.pdf and S4 Fig.
(PDF)

S5 Fig. S5 Fig PLOS ONE-3rd revised.pdf and S5 Fig.
(PDF)

S6 Fig. S6 Fig PLOS ONE-3rd revised.pdf and S6 Fig.
(PDF)

S7 Fig. S7 Fig PLOS ONE-3rd revised.pdf and S7 Fig.
(PDF)

Author Contributions

References

1. Kim YS, Sainz RD, Molenaar P, Summers RJ. Characterization of β_1- and β_2-adrenoceptors in rat skeletal muscles. Biochem Pharmacol. 1991; 42(9):1783–1789. PMID: 1681810

2. Woo AY, Xiao RP. β-Adrenergic receptor subtype signaling in heart: from bench to bedside. Acta Pharmacol Sin. 2012; 33(3):335–341. https://doi.org/10.1038/aps.2011.201 PMID: 22286918

3. Communal C, Singh K, Sawyer DB, Colucci WS. Opposing effects of β_1- and β_2-adrenergic receptors on cardiac myocyte apoptosis: role of a pertussis toxin-sensitive G protein. Circulation. 1999; 100 (22):2210–2212. PMID: 10577992

4. Morisco C, Zebrowski DC, Vatner DE, Vatner SF, Sadoshima J. β_1-adrenergic cardiac hypertrophy is mediated primarily by the β_1-subtype in the rat heart. J Mol Cell Cardiol. 2001; 33(3):561–573. https://doi.org/10.1006/jmcc.2000.1332 PMID: 11181023

5. Zhu WZ, Wang SQ, Chakir K, Yang D, Zhang T, Brown JH, et al. Linkage of β_1-adrenergic stimulation to apoptotic heart cell death through protein kinase A-independent activation of Ca^{2+}/calmodulin kinase II. J Clin Invest. 2003; 111(5):617–625. https://doi.org/10.1172/JCI16326 PMID: 12618516

6. Xu XY, Nie Y, Wang FF, Bai Y, Lv ZZ, Zhang YY, et al. Growth differentiation factor (GDF)-15 blocks norepinephrine-induced myocardial hypertrophy via a novel pathway involving inhibition of epidermal growth factor receptor transactivation. J Biol Chem. 2014; 289(14):10084–10094. https://doi.org/10.1074/jbc.M113.516278 PMID: 24554716

7. Iwai-Kanai E, Hasegawa K, Araki M, Kakita T, Morimoto T, Sasayama S. α- and β-adrenergic pathways differentially regulate cell type-specific apoptosis in rat cardiac myocytes. Circulation. 1999; 100 (3):305–311. PMID: 10411857

8. Bisognano JD, Weinberger HD, Bohlmeyer TJ, Pende A, Raynolds MV, Sastravaha A, et al. Myocardial-directed overexpression of the human β_1-adrenergic receptor in transgenic mice. J Mol Cell Cardiol. 2000; 32(5):817–830. https://doi.org/10.1006/jmcc.2000.1123 PMID: 10775486

9. Zhu WZ, Zheng M, Koch WJ, Lefkowitz RJ, Kobilka BK, Xiao RP. Dual modulation of cell survival and cell death by β_2-adrenergic signaling in adult mouse cardiac myocytes. Proc Natl Acad Sci U S A. 2001; 98(4):1607–1612. https://doi.org/10.1073/pnas.98.4.1607 PMID: 11171998

10. Chesley A, Lundberg MS, Asai T, Xiao RP, Ohtani S, Lakatta EG, et al. The β_2-adrenergic receptor delivers an antiapoptotic signal to cardiac myocytes through Gi-dependent coupling to phosphatidylinositol 3'-kinase. Circ Res. 2000; 87(12):1172–1179. PMID: 11110775

11. Ohnuki Y, Umeki D, Mototani Y, Jin H, Cai W, Shiozawa K, et al. Role of cyclic AMP sensor Epac1 in masseter muscle hypertrophy and myosin heavy chain transition induced by β_2-adrenoceptor stimulation. J Physiol. 2014; 592(24):5461–5475. https://doi.org/10.1113/jphysiol.2014.282996 PMID: 25344550

12. Ohnuki Y, Umeki D, Mototani Y, Shiozawa K, Nariyama M, Ito A, et al. Role of phosphodiesterase 4 expression in the Epac1 signaling-dependent skeletal muscle hypertrophic action of clenbuterol. Physiol Rep. 2016; 4(10):e12791. https://doi.org/10.14814/phy2.12791 PMID: 27207782

13. Ohnuki Y, Umeki D, Cai W, Kawai N, Mototani Y, Shiozawa K, et al. Role of masseter muscle β2-adrenergic signaling in regulation of muscle activity, myosin heavy chain transition, and hypertrophy. J Pharmacol Sci. 2013; 123(1):36–46. PMID: 23985574

14. Sirvent P, Douillard A, Galbes O, Ramonatxo C, Py G, Candau R, et al. Effects of chronic administration of clenbuterol on contractile properties and calcium homeostasis in rat extensor digitorum longus muscle. PLoS One. 2014; 9(6):e100281. https://doi.org/10.1371/journal.pone.0100281 PMID: 24971566

15. Dodd SL, Powers SK, Vrabas IS, Criswell D, Stetson S, Hussain R, et al. Effects of clenbuterol on contractile and biochemical properties of skeletal muscle. Med Sci Sports Exerc. 1996; 28(6):669–676. PMID: 8784754

16. Sciarretta S, Forte M, Frati G, Sadoshima J. New insights into the role of mTOR signaling in the cardiovascular system. Circ Res. 2018; 122(3):489–505. https://doi.org/10.1161/CIRCRESAHA.117.311147 PMID: 29420210

17. Sato M, Dehvari N, Oberg AI, Dallner OS, Sandstrom AL, Olsen JM, et al. Improving type 2 diabetes through a distinct adrenergic signaling pathway involving mTORC2 that mediates glucose uptake in skeletal muscle. Diabetes. 2014; 63(12):4115–4129. https://doi.org/10.2337/db13-1860 PMID: 25008179

18. Eshima H, Tamura Y, Kakehi S, Nakamura K, Kurebayashi N, Murayama T, et al. Dysfunction of muscle contraction with impaired intracellular Ca^{2+} handling in skeletal muscle and the effect of exercise training in male db/db mice. J Appl Physiol. 2019; 126(1):170–182. https://doi.org/10.1152/japplphysiol.00048.2018 PMID: 30433865

19. Huang X, Liu S, Wu D, Cheng Y, Han H, Wang K, et al. Facilitated Ca^{2+} homeostasis and attenuated myocardial autophagy contribute to alleviation of diabetic cardiomyopathy after bariatric surgery. Am J

Physiol Heart Circ Physiol. 2018; 315(5):H1258–H1268. https://doi.org/10.1152/ajpheart.00274.2018 PMID: 30141985

20. Periasamy M, Kalyanasundaram A. SERCA pump isoforms: their role in calcium transport and disease. Muscle Nerve. 2007; 35(4):430–442. https://doi.org/10.1002/mus.20745 PMID: 17286271

21. Koss KL, Kranias EG. Phospholamban: a prominent regulator of myocardial contractility. Circ Res. 1996; 79(6):1059–1063. PMID: 8943944

22. Okumura S, Fujita T, Cai W, Jin M, Namekata I, Mototani Y, et al. *Epac1*-dependent phospholamban phosphorylation mediates the cardiac response to stresses. J Clin Invest. 2014; 124(6):2785–2801. https://doi.org/10.1172/JCI64784 PMID: 24892712

23. Haghighi K, Bidwell P, Kranias EG. Phospholamban interactome in cardiac contractility and survival: A new vision of an old friend. J Mol Cell Cardiol. 2014; 77:160–167. https://doi.org/10.1016/j.yjmcc.2014.10.005 PMID: 25451386

24. Pattison JS, Waggoner JR, James J, Martin L, Gulick J, Osinska H, et al. Phospholamban overexpression in transgenic rabbits. Transgenic Res. 2008; 17(2):157–170. https://doi.org/10.1007/s11248-007-9139-2 PMID: 17882530

25. Fajardo VA, Bombardier E, McMillan E, Tran K, Wadsworth BJ, Gamu D, et al. Phospholamban overexpression in mice causes a centronuclear myopathy-like phenotype. Dis Model Mech. 2015; 8(8):999–1009. https://doi.org/10.1242/dmm.020859 PMID: 26035394

26. Vincelette J, Martin-McNulty B, Vergona R, Sullivan ME, Wang YX. Reduced cardiac functional reserve in apolipoprotein E knockout mice. Transl Res. 2006; 148(1):30–36. https://doi.org/10.1016/j.lab.2006.03.007 PMID: 16887496

27. Santulli G, Lombardi A, Sorriento D, Anastasio A, Del Giudice C, Formisano P, et al. Age-related impairment in insulin release: the essential role of β_2-adrenergic receptor. Diabetes. 2012; 61(3): 692–701. https://doi.org/10.2337/db11-1027 PMID: 22315324

28. Ryall JG, Gregorevic P, Plant DR, Sillence MN, Lynch GS. β_2-agonist fenoterol has greater effects on contractile function of rat skeletal muscles than clenbuterol. Am J Physiol Regul Integr Comp Physiol. 2002; 283(6): R1386–R1394. https://doi.org/10.1152/ajpregu.00324.2002 PMID: 12388476

29. Goodman CA, Frey JW, Mabrey DM, Jacobs BL, Lincoln HC, You JS, et al. The role of skeletal muscle mTOR in the regulation of mechanical load-induced growth. J Physiol. 2011; 589(Pt 22):5485–5501. https://doi.org/10.1113/jphysiol.2011.218255 PMID: 21946849

30. Bruusgaard JC, Egner IM, Larsen TK, Dupre-Aucouturier S, Desplanches D, Gundersen K, et al. No change in myonuclear number during muscle unloading and reloading. J Appl Physiol. 2012; 113 (2):290–296. https://doi.org/10.1152/japplphysiol.00436.2012 PMID: 22582213

31. Kiliaridis S, Engstrom C, Thilander B. Histochemical analysis of masticatory muscle in the growing rat after prolonged alteration in the consistency of the diet. Arch Oral Biol. 1988; 33(3):187–193. PMID: 3178538

32. Okumura S, Takagi G, Kawabe J, Yang G, Lee MC, Hong C, et al. Disruption of type 5 adenylyl cyclase gene preserves cardiac function against pressure overload. Proc Natl Acad Sci U S A. 2003; 100(17): 9986–9990. https://doi.org/10.1073/pnas.1733772100 PMID: 12904575

33. Yan J, Thomson JK, Wu X, Zhao W, Pollard AE, Ai X. Novel methods of automated quantification of gap junction distribution and interstitial collagen quantity from animal and human atrial tissue sections. PLoS One. 2014; 9(8):e104357. https://doi.org/10.1371/journal.pone.0104357 PMID: 25105669

34. Stromp TA, Spear TJ, Holtkamp RM, Andres KN, Kaine JC, Alghuraibawi WH, et al. Quantitative gadolinium-free cardiac fibrosis imaging in end stage renal disease patients reveals a longitudinal correlation with structural and functional decline. Sci Rep. 2018; 8(1):16972. https://doi.org/10.1038/s41598-018-35394-4 PMID: 30451960

35. Cai W, Fujita T, Hidaka Y, Jin H, Suita K, Prajapati R, et al. Disruption of Epac1 protects the heart from adenylyl cyclase type 5-mediated cardiac dysfunction. Biochem Biophys Res Commun. 2016; 475:1–7. https://doi.org/10.1016/j.bbrc.2016.04.123 PMID: 27117748

36. Sano M, Minamino T, Toko H, Miyauchi H, Orimo M, Qin Y, et al. p53-induced inhibition of Hif-1 causes cardiac dysfunction during pressure overload. Nature. 2007; 446(7134): 444–448. https://doi.org/10.1038/nature05602 PMID: 17334357

37. Ohnuki Y, Nishimura S, Sugiura S, Saeki Y. Phosphorylation status of regulatory proteins and functional characteristics in myocardium of dilated cardiomyopathy of Syrian hamsters. J Physiol Sci. 2008; 58 (1):15–20. https://doi.org/10.2170/physiolsci.RP012807 PMID: 18177543

38. Saeki Y, Kato C, Horikoshi T, Yanagisawa K. Mechanical properties of glycerinated guinea-pig temporal and masseter muscles. Arch Oral Biol. 1984; 29:663–668. PMID: 6594098

39. Yu H, He Y, Zhang X, Peng Z, Yang Y, Zhu R, et al. The rat IgGFcγBP and Muc2 C-terminal domains and TFF3 in two intestinal mucus layers bind together by covalent interaction. PLoS One. 2011; 6(5): e20334. https://doi.org/10.1371/journal.pone.0020334 PMID: 21629776

40. Okumura S, Kawabe J, Yatani A, Takagi G, Lee MC, Hong C, et al. Type 5 adenylyl cyclase disruption alters not only sympathetic but also parasympathetic and calcium-mediated cardiac regulation. Circ Res. 2003; 93(4):364–371. https://doi.org/10.1161/01.RES.0000086986.35568.63 PMID: 12869393

41. Okumura S, Tsunematsu T, Bai Y, Jiao Q, Ono S, Suzuki S, et al. Type 5 adenylyl cyclase plays a major role in stabilizing heart rate in response to microgravity induced by parabolic flight. J Appl Physiol. 2008; 105:173–179. https://doi.org/10.1152/japplphysiol.01166.2007 PMID: 18450980

42. Kitakaze T, Sakamoto T, Kitano T, Inoue N, Sugihara F, Harada N, et al. The collagen derived dipeptide hydroxyprolyl-glycine promotes C2C12 myoblast differentiation and myotube hypertrophy. Biochem Biophys Res Commun. 2016; 478(3):1292–1297. https://doi.org/10.1016/j.bbrc.2016.08.114 PMID: 27553280

43. Riccardi C, Nicoletti I. Analysis of apoptosis by propidium iodide staining and flow cytometry. Nat Protoc. 2006; 1(3):1458–1461. https://doi.org/10.1038/nprot.2006.238 PMID: 17406435

44. Wannenes F, Magni L, Bonini M, Dimauro I, Caporossi D, Moretti C, et al. In vitro effects of beta-2 ago-nists on skeletal muscle differentiation, hypertrophy, and atrophy. World Allergy Organ J. 2012; 5 (6):66–72. https://doi.org/10.1097/WOX.0b013e31825eff8b PMID: 23283108

45. Dostanic S, Servant N, Wang C, Chalifour LE. Chronic β-adrenoreceptor stimulation in vivo decreased Bcl-2 and increased Bax expression but did not activate apoptotic pathways in mouse heart. Can J Phy-siol Pharmacol. 2004; 82:167–174. https://doi.org/10.1139/y03-134 PMID: 15052282

46. Gaussin V, Tomlinson JE, Depre C, Engelhardt S, Antos CL, Takagi G, et al. Common genomic response in different mouse models of β-adrenergic-induced cardiomyopathy. Circulation. 2003; 108 (23):2926–2933. https://doi.org/10.1161/01.CIR.0000101922.18151.7B PMID: 14623810

47. Tummers B, Green DR. Caspase-8: regulating life and death. Immunol Rev. 2017; 277(1): 76–89. https://doi.org/10.1111/imr.12541 PMID: 28462525

48. Ballak SB, Buse-Pot T, Harding PJ, Yap MH, Deldicque L, de Haan A, et al. Blunted angiogenesis and hypertrophy are associated with increased fatigue resistance and unchanged aerobic capacity in old overloaded mouse muscle. Age. 2016; 38(2):39. https://doi.org/10.1007/s11357-016-9894-1 PMID: 26970774

49. Hanft LM, Emter CA, McDonald KS. Cardiac myofibrillar contractile properties during the progression from hypertension to decompensated heart failure. Am J Physiol Heart Circ Physiol. 2017; 313(1): H103–H113. https://doi.org/10.1152/ajpheart.00069.2017 PMID: 28455288

50. Ohnuki Y, Saeki Y. Jaw-opening muscle contracts more economically than jaw-closing muscle in rat. Arch Oral Biol. 2008; 53(2):193–198. https://doi.org/10.1016/j.archoralbio.2007.09.004 PMID: 18028867

51. Zakhary DR, Moravec CS, Stewart RW, Bond M. Protein kinase A (PKA)-dependent troponin-I phos-phorylation and PKA regulatory subunits are decreased in human dilated cardiomyopathy. Circulation. 1999; 99(4):505–510. PMID: 9927396

52. Tikunova S, Belevych N, Doan K, Reiser PJ. Desensitizing mouse cardiac troponin C to calcium con-verts slow muscle towards a fast muscle phenotype. J Physiol. 2018; 596(19): 4651–4663. https://doi.org/10.1113/JP276296 PMID: 29992562

53. Cazorla O, Lucas A, Poirier F, Lacampagne A, Lezoualc'h F. The cAMP binding protein Epac regulates cardiac myofilament function. Proc Natl Acad Sci U S A. 2009; 10614144–14149.

54. Shioi T, McMullen JR, Kang PM, Douglas PS, Obata T, Franke TF, et al. Akt/protein kinase B promotes organ growth in transgenic mice. Mol Cell Biol. 2002; 22(8):2799–2809. https://doi.org/10.1128/MCB.22.8.2799-2809.2002 PMID: 11909972

55. Okumura S, Vatner DE, Kurotani R, Bai Y, Gao S, Yuan Z, et al. Disruption of type 5 adenylyl cyclase enhances desensitization of cyclic adenosine monophosphate signal and increases Akt signal with chronic catecholamine stress. Circulation. 2007; 116:1776–1783. https://doi.org/10.1161/CIRCULATIONAHA.107.698662 PMID: 17893275

56. Lv T, Du Y, Cao N, Zhang S, Gong Y, Bai Y, et al. Proliferation in cardiac fibroblasts induced by β1-adre-noceptor autoantibody and the underlying mechanisms. Sci Rep 6:32430. https://doi.org/10.1038/srep32430 PMID: 27577254

57. Leicht M, Briest W, Zimmer HG. Regulation of norepinephrine-induced proliferation in cardiac fibro-blasts by interleukin-6 and p42/p44 mitogen activated protein kinase. Mol Cell Biochem. 2003; 243(1–2):65–72. PMID: 12619890

58. Grumati P, Bonaldo P. Autophagy in skeletal muscle homeostasis and in muscular dystrophies. Cells. 2012; 1(3):325–345. https://doi.org/10.3390/cells1030325 PMID: 24710479

59. Kanamori H, Takemura G, Goto K, Maruyama R, Tsujimoto A, Ogino A, et al. The role of autophagy emerging in postinfarction cardiac remodelling. Cardiovasc Res. 2011; 91(2):330–339. https://doi.org/10.1093/cvr/cvr073 PMID: 21406597

60. Fernandez-Sola J, Planavila Porta A. New treatment strategies for alcohol-induced heart damage. Int J Mol Sci. 2016; 17(10):E1651. https://doi.org/10.3390/ijms17101651 PMID: 27690014

61. Xie WY, Zhou XD, Yang J, Chen LX, Ran DH. Inhibition of autophagy enhances heat-induced apoptosis in human non-small cell lung cancer cells through ER stress pathways. Arch Biochem Biophys. 2016; 607:55–66. https://doi.org/10.1016/j.abb.2016.08.016 PMID: 27565443

62. Maier LS, Zhang T, Chen L, DeSantiago J, Brown JH, Bers DM. Transgenic CaMKIIδ$_C$ overexpression uniquely alters cardiac myocyte Ca^{2+} handling: reduced SR Ca^{2+} load and activated SR Ca^{2+} release. Circ Res. 2003; 92(8): 904–911. https://doi.org/10.1161/01.RES.0000069685.20258.F1 PMID: 12676813

63. Sossalla S, Fluschnik N, Schotola H, Ort KR, Neef S, Schulte, et al. Inhibition of elevated Ca^{2+}/calmodulin-dependent protein kinase II improves contractility in human failing myocardium. Circ Res. 2010; 107 (9):1150–1161. https://doi.org/10.1161/CIRCRESAHA.110.220418 PMID: 20814023

64. Ravel-Chapuis A, Belanger G, Cote J, Michel RN, Jasmin BJ. Misregulation of calcium-handling proteins promotes hyperactivation of calcineurin-NFAT signaling in skeletal muscle of DM1 mice. Hum Mol Genet. 2017; 26(12):2192–2206. https://doi.org/10.1093/hmg/ddx109 PMID: 28369518

65. Murphy RM. Calpains, skeletal muscle function and exercise. Clin Exp Pharmacol Physiol. 2010; 37 (3):385–391. https://doi.org/10.1111/j.1440-1681.2009.05310.x PMID: 19793101

66. Tothova J, Blaauw B, Pallafacchina G, Rudolf R, Argentini C, Reggiani C, et al. NFATc1 nucleocytoplasmic shuttling is controlled by nerve activity in skeletal muscle. J Cell Sci. 2006; 119(Pt 8):1604–1611. https://doi.org/10.1242/jcs.02875 PMID: 16569660

67. El-Armouche A, Wittkopper K, Degenhardt F, Weinberger F, Didie M, Melnychenko I, et al. Phosphatase inhibitor-1-deficient mice are protected from catecholamine-induced arrhythmias and myocardial hypertrophy. Cardiovasc Res. 2008; 80(3):396–406. https://doi.org/10.1093/cvr/cvn208 PMID: 18689792

68. Soppa GK, Smolenski RT, Latif N, Yuen AH, Malik A, Karbowska J, et al. Effects of chronic administration of clenbuterol on function and metabolism of adult rat cardiac muscle. Am J Physiol Heart Circ Physiol. 2005; 288(3):H1468–H1476. https://doi.org/10.1152/ajpheart.00624.2004 PMID: 15528231

69. Engelhardt S, Hein L, Wiesmann F, Lohse MJ. Progressive hypertrophy and heart failure in β$_1$-adrenergic receptor transgenic mice. Proc Natl Acad Sci U S A. 1999; 96(12):7059–7064. PMID: 10359838

70. Xiao D, Dasgupta C, Chen M, Zhang K, Buchholz J, Xu Z, et al. Inhibition of DNA methylation reverses norepinephrine-induced cardiac hypertrophy in rats. Cardiovasc Res. 2014; 101(3):373–382. https://doi.org/10.1093/cvr/cvt264 PMID: 24272874

71. Tsuneyoshi H, Oriyanhan W, Kanemitsu H, Shiina R, Nishina T, Matsuoka S, et al. Does the β$_2$-agonist clenbuterol help to maintain myocardial potential to recover during mechanical unloading? Circulation. 2005; 112(Supp I):I51–I56.

72. Karuppagounder V, Arumugam S, Thandavarayan RA, Pitchaimani V, Sreedhar R, Afrin R, et al. Naringenin ameliorates daunorubicin induced nephrotoxicity by mitigating AT1R, ERK1/2-NFκB p65 mediated inflammation. Int Immunopharmacol. 2015; 28:154–159. https://doi.org/10.1016/j.intimp.2015.05.050 PMID: 26072060

73. Bi QR, Hou JJ, Qi P, Ma CH, Feng RH, Yan BP, et al. TXNIP/TRX/NF-κB and MAPK/NF-κB pathways involved in the cardiotoxicity induced by Venenum Bufonis in rats. Sci Rep. 2016; 6:22759. https://doi.org/10.1038/srep22759 PMID: 26961717

74. McMullen JR, Shioi T, Zhang L, Tarnavski O, Sherwood MC, Dorfman AL, et al. Deletion of ribosomal S6 kinases does not attenuate pathological, physiological, or insulin-like growth factor 1 receptor-phosphoinositide 3-kinase-induced cardiac hypertrophy. Mol Cell Biol. 2004; 24:6231–6240. https://doi.org/10.1128/MCB.24.14.6231-6240.2004 PMID: 15226426

75. Brandt N, Nielsen L, Thiellesen Buch B, Gudiksen A. Impact of β-adrenergic signaling in PGC-1α-mediated adaptations in mouse skeletal muscle. Am J Physiol Endocrinol Metab. 2018; 314(1): E1–E20. https://doi.org/10.1152/ajpendo.00082.2017 PMID: 28874356

76. Laplante M, Sabatini DM. mTOR signaling in growth control and disease. Cell. 2012; 149(2): 274–293. https://doi.org/10.1016/j.cell.2012.03.017 PMID: 22500797

77. Copp J, Manning G, Hunter T. TORC-specific phosphorylation of mammalian target of rapamycin (mTOR): phospho-Ser2481 is a marker for intact mTOR signaling complex 2. Cancer Res. 2009; 69 (5):1821–1827. https://doi.org/10.1158/0008-5472.CAN-08-3014 PMID: 19244117

78. Luo W, Grupp IL, Harrer J, Ponniah S, Grupp G, Duffy JJ, et al. Targeted ablation of the phospholamban gene is associated with markedly enhanced myocardial contractility and loss of β-agonist stimulation. Circ Res. 1994; 75(3):401–409. PMID: 8062415

79. Kuschel M, Karczewski P, Hempel P, Schlegel WP, Krause EG, Bartel S, et al. Ser16 prevails over Thr17 phospholamban phosphorylation in the beta-adrenergic regulation of cardiac relaxation. Am J

Physiol. 1999; 276: H1625–H1633. https://doi.org/10.1152/ajpheart.1999.276.5.H1625 PMID: 10330247

80. Sordahl LA, McCollum WB, Wood WG, Schwartz A. Mitochondria and sarcoplasmic reticulum function in cardiac hypertrophy and failure. Am J Physiol. 1973; 224(3):497–502. https://doi.org/10.1152/ajplegacy.1973.224.3.497 PMID: 4266238

81. Whitmer JT, Kumar P, Solaro RJ. Calcium transport properties of cardiac sarcoplasmic reticulum from cardiomyopathic Syrian hamsters (BIO 53.58 and 14.6): evidence for a quantitative defect in dilated myopathic hearts not evident in hypertrophic hearts. Circ Res. 1988; 62(1):81–85. PMID: 2961480

82. Minamisawa S, Hoshijima M, Chu G, Ward CA, Frank K, Gu Y, et al. Chronic phospholamban-sarco-plasmic reticulum calcium ATPase interaction is the critical calcium cycling defect in dilated cardiomyop-athy. Cell. 1999; 99(3):313–322. PMID: 10555147

83. Sato Y, Kiriazis H, Yatani A, Schmidt AG, Hahn H, Ferguson DG, et al. Rescue of contractile parame-ters and myocyte hypertrophy in calsequestrin overexpressing myocardium by phospholamban abla-tion. J Biol Chem. 2011; 276(12):9392–9399.

84. Cross HR, Kranias EG, Murphy E, Steenbergen C. Ablation of PLB exacerbates ischemic injury to a lesser extent in female than male mice: protective role of NO. Am J Physiol Heart Circ Physiol. 2003; 284:H683–H690. https://doi.org/10.1152/ajpheart.00567.2002 PMID: 12388218

85. Zhang T, Guo T, Mishra S, Dalton ND, Kranias EG, Peterson KL, et al. Phospholamban ablation res-cues sarcoplasmic reticulum Ca^{2+} handling but exacerbates cardiac dysfunction in CaMKIIδ$_C$ trans-genic mice. Circ Res. 2010; 106(2):354–362. https://doi.org/10.1161/CIRCRESAHA.109.207423 PMID: 19959778

86. Belfrage E. Comparison of β-adrenoceptors mediating vasodilatation in canine subcutaneous adipose tissue and skeletal muscle. Acta Physiol Scand. 1978; 102(4):469–476. https://doi.org/10.1111/j.1748-1716.1978.tb06095.x PMID: 26166

87. Ishii H, Niioka T, Izumi H. Circulating adrenaline released by sympathoadrenal activation elicits acute vasodilatation in the rat masseter muscle. Arch Oral Biol. 2009; 54(5):486–494. https://doi.org/10.1016/j.archoralbio.2009.01.012 PMID: 19329107

88. Banquet S, Delannoy E, Agouni A, Dessy C, Lacomme S, Hubert F, et al. Role of G$_{i/o}$-Src kinase-PI3K/Akt pathway and caveolin-1 in β$_2$-adrenoceptor coupling to endothelial NO synthase in mouse pulmo-nary artery. Cell Signal. 2011; 23(7):1136–1143. https://doi.org/10.1016/j.cellsig.2011.02.008 PMID: 21385608

89. Lee TJ. Sympathetic modulation of nitrergic neurogenic vasodilation in cerebral arteries. Jpn J Pharma-col. 2002; 88(1):26–31. PMID: 11859855

90. Verges S, Rupp T, Jubeau M, Wuyam B, Esteve F, Levy P, et al. Cerebral perturbations during exercise in hypoxia. Am J Physiol Regul Integr Comp Physiol. 2012; 302(8): R903–R916. https://doi.org/10.1152/ajpregu.00555.2011 PMID: 22319046

91. Grunheid T, Langenbach GE, Zentner A, Van Eijden TM. Duty time of rabbit jaw muscles varies with the number of activity bursts. J Dent Res. 2006; 85(12):1112–1117. https://doi.org/10.1177/154405910608501209 PMID: 17122164

92. Iida T, Sakayanagi M, Svensson P, Komiyama O, Hirayama T, Kaneda T, et al. Influence of periodontal afferent inputs for human cerebral blood oxygenation during jaw movements. Exp Brain Res. 2012; 216: 375–384. https://doi.org/10.1007/s00221-011-2941-3 PMID: 22101493

93. Lynch GS, Ryall JG. Role of β-adrenoceptor signaling in skeletal muscle: implications for muscle wast-ing and disease. Physiol Rev. 2008; 88(2):729–767. https://doi.org/10.1152/physrev.00028.2007 PMID: 18391178